Construction and Local Equivalence of Dual-Unitary Operators: From Dynamical Maps to Quantum Combinatorial Designs

Suhail Ahmad Rather,[1,*] S. Aravinda,[2,†] and Arul Lakshminarayan[1]

[1] *Department of Physics, Indian Institute of Technology Madras, Chennai 600036, India*

[2] *Department of Physics, Indian Institute of Technology Tirupati, Tirupati 517619, India*

(Received 4 June 2022; revised 16 October 2022; accepted 16 November 2022; published 20 December 2022)

While quantum circuits built from two-particle dual-unitary (maximally entangled) operators serve as minimal models of typically nonintegrable many-body systems, the construction and characterization of dual-unitary operators themselves are only partially understood. A nonlinear map on the space of unitary operators has been proposed in *Phys. Rev. Lett.* **125**, 070501 (2020) that results in operators being arbitrarily close to dual unitaries. Here, we study the map analytically for the two-qubit case describing the basins of attraction, fixed points, and rates of approach to dual unitaries. A subset of dual-unitary operators having maximum entangling power are 2-unitary operators or perfect tensors and these are equivalent to four-party absolutely maximally entangled states. It is known that they only exist if the local dimension is larger than $d = 2$. We use the nonlinear map, and introduce stochastic variants of it, to construct explicit examples of new dual and 2-unitary operators. A necessary criterion for their local unitary equivalence to distinguish classes is also introduced and used to display various concrete results and a conjecture in $d = 3$. It is known that orthogonal Latin squares provide a "classical combinatorial design" for constructing permutations that are 2-unitary. We extend the underlying design from classical to genuine quantum ones for general dual-unitary operators and give an example of what might be the smallest-sized genuinely quantum design of a 2-unitary in $d = 4$.

DOI: 10.1103/PRXQuantum.3.040331

I. INTRODUCTION

In recent years a major research trend has been to use the tools of quantum information theory to understand the puzzles of quantum many-body physics. The typically complex entanglement structure of many-body states drives cross fertilization across various fields of research in physics. Particularly in the areas of condensed-matter physics and string theory, quantum information theory continues to play an exciting role in creating new avenues of understanding [1–4].

Quantum computers allow the realization of the vision of Feynman [5] on the efficient simulation of physical systems [6]. In the present era of noisy-intermediate-scale quantum (NISQ) [7] computing, such simulations become realistic [8]. The universality of quantum computing allows simulation of any quantum system, where quantum circuits are built using unitary operators or gates acting on single-particle and two-particle subsystems. A quantum computer is itself a controllable quantum many-body system. Traditional approaches involve studying the properties of systems based on the Hamiltonian evolution and spectra. At this juncture, it is important to understand the properties of quantum many-body systems from the quantum circuit formalism and to contrast that with the traditional studies.

Quantum advantage using random unitary circuits has been explored in recent experiments using Google's "Sycamore" processor [9] and "Zuchongzhi 2.0" [10]. Similar models are used in studies of entanglement evolution in many-body quantum systems, in which the random unitary gates act on nearest neighbors [11–15]. Quantum circuits in arbitrary local dimensions, without any random interactions, have been proposed as elegant minimal models that can span the gamut of integrable to fully chaotic quantum many-body systems [16–19]. These quantum circuits have a special "duality" property in that the evolution operator in the spatial as well as in the temporal direction of the circuit is governed by unitary dynamics. The origin of this duality lies in the two-particle unitary gates being *dual unitary* [17]. This duality facilitates an analytical treatment of many quantities such as two-point correlation

*suhailmushtaq@physics.iitm.ac.in

†aravinda@iittp.ac.in

functions, the spectral form factor, operator entanglement, out-of-time-order correlators, and the exact study of the entanglement dynamics [17,18,20–35]. The two-particle unitary from which the circuit is built plays a significant role in the following and is an operator in d^2-dimensional space, where the local dimension is d and is typically denoted as U.

On the other hand, entanglement of unitary operators, similar to states, has been studied from the early days of quantum information theory [36–45]. Quantities such as operator entanglement [37], the entangling power [36], and the complexity of an operator [46] are a few measures that quantify the nonlocal properties of unitary operators. Operator entanglement measures how entangled an operator is when viewed as a vector in a product vector space. It has been identified that a unitary operator is dual unitary if and only if it has maximum possible operator entanglement [47]. The entangling power quantifies the average entanglement produced by a bipartite unitary operator acting on an ensemble of pure product states. A special subclass of dual-unitary operators are those having the maximum possible entangling power allowed by local dimensions. These are the same operators that have been referred to variously as 2-unitary [48] or perfect tensors [49].

The exactly calculable two-point correlation functions in dual-unitary circuits enable the characterization of the many-body system in terms of an ergodic hierarchy, from ergodic to Bernoulli through mixing [17,50]. It is identified that the dual-unitary circuit is Bernoulli when correlations instantly decay, if and only if the two-particle unitary operator has maximum entangling power [50]. Additionally, a sufficient condition for the many-body circuit to show the mixing behavior is derived as a function of the entangling power [50]. These results establish a close connection between the entangling properties of the two-particle unitary operators from which the many-body quantum circuits are built and the dynamical nature of the many-body systems.

Let the Schmidt form of a bipartite pure quantum state be $|\psi\rangle_{AB} = \sum_{i=0}^{d-1} \sqrt{\lambda_i}\,|ii\rangle\,/\sqrt{d}$, where d is the local Hilbert-space dimension. Setting $\lambda_i = 1$ for all i in this expansion results in $|\Phi\rangle = \sum_{i=1}^{d} |ii\rangle\,/\sqrt{d}$, which is a maximally entangled state—in fact, the one that is closest to $|\psi_{AB}\rangle$. Any set of orthonormal bases in the subspaces constructs such maximally entangled states.

In contrast, the construction of maximally entangled unitary operators does not follow from orthonormal operator bases. Let us express a unitary operator in operator Schmidt form, $U = \sum_{j=1}^{d^2} \sqrt{\lambda_j} X_j \otimes Y_j$, $\mathrm{tr}(X_j^\dagger X_k) = \mathrm{tr}(Y_j^\dagger Y_k) = \delta_{jk}$, and $\lambda_j \geq 0$. U is maximally entangled or dual unitary if and only if $\lambda_i = 1$ for all i. However, the constraint of unitarity is stronger than the constraint of normalization on the state and this imposes complex conditions on the Schmidt matrices X_j and Y_j. Thus simply assigning $\lambda_i = 1$ for all i does not retain unitarity, although it does result in a maximally entangled operator. This makes it hard to analytically construct dual-unitary operators. Construction of maximally entangled unitaries has been discussed at least as early as in Ref. [51].

If the local dimension is $d = 2$, namely for qubits, all possible dual-unitary operators can be parametrized using the Cartan decomposition [17]. There are no 2-unitary or perfect tensors in this case. While a complete parametrization of dual-unitary operators for $d > 2$ is not known, many classes and examples have been examined and used thus far. The SWAP or flip operator is a simple example of a dual-unitary operator. The discrete Fourier transform in d^2 dimensions maximizes operator entanglement [52,53] and is hence also dual unitary. However, the SWAP has zero entangling power, while the Fourier transform has a finite value. Diagonal and block diagonal operators, along with the SWAP gate, can be used to construct a dual-unitary operator [50,54]. These have limited entangling power and in particular cannot reach the maximum value [50]. The dual-unitary operators introduced recently in Ref. [55] are also bounded by the entangling power of diagonal unitary operators.

A numerical iterative algorithm that produces unitary operators that are arbitrarily close to being dual unitary has been presented in Ref. [47]. This algorithm can yield dual-unitary operators with a wide range of entangling powers, especially exceeding the bound corresponding to block-diagonal-based constructions. Remarkably, the numerical algorithm can also yield exact analytical forms for dual-unitary operators [50] and several other examples, including new 2-unitaries, are displayed further below. A slightly modified algorithm has been used to positively settle an open problem on the existence of four-party absolutely maximally entangled (AME) states of local dimension six [56] (see also Ref. [57], for an elaborate discussion of the solution). AME states are genuinely entangled multipartite pure states that have maximal entanglement in all bipartitions [58]. Thus an AME state of N qudits, each of dimension d, denoted as AME(N, d) has all subsystems of size $\lfloor N/2 \rfloor$ maximally mixed.

The numerical algorithm acts generically as a dynamical map in the space of unitary operators. These are thus high-dimensional dynamical systems that deserve to be studied in their own right. In this work, we study the fixed-point structure of the map. In particular, for the case of two qubits, an explicit analytical form of the map is derived. This enables the derivation of dynamical characteristics such as the rate of approach to attractors that are dual-unitary operators. A variety of dynamical behaviors have been observed: (i) power-law approaches to the SWAP gate and (ii) an exponential approach to other dual-unitary gates, with a rate that diverges for the maximally entangling case of the double-controlled-NOT (DCNOT) gate.

Due to operator-state isomorphism, a 2-unitary operator is equivalent to a four-party AME state [48]. There are various ways of constructing AME states in which quantum combinatorial designs are used [48,59]. Since 2-unitaries are a subset of dual unitaries, a less restrictive combinatorial design underlying dual-unitary operators that are permutations has been found in Ref. [50]. In this work, we extend such combinatorial designs to dual-unitary operators going beyond permutations. We define *stochastic* dynamical maps capable of generating such structured dual-unitary operators.

Apart from dual-unitary operators, the maps presented in Ref. [47] can be used to generate infinitely many 2-unitaries for $d > 2$. An important question now arises if the 2-unitaries so obtained are local unitarily (LU) equivalent to each other and to 2-unitary permutations of the same size. Two bipartite unitary operators, U and U', on $\mathcal{H}_d \otimes \mathcal{H}_d$ are said to local unitarily equivalent, denoted by $U \overset{\text{LU}}{\sim} U'$, if there exist single-qudit unitary gates u_1, u_2, v_1, and v_2 such that

$$U' = (u_1 \otimes u_2)U(v_1 \otimes v_2). \tag{1}$$

However, as far as we know, there is no general procedure to identify LU-equivalent unitary operators, apart from the case of two qubits [45]. This problem becomes acute when the operators concerned, such as the 2-unitaries, have the same entangling powers. In this work, we address this question by proposing a necessary criterion for LU equivalence between bipartite unitary operators that can potentially also work in the case of 2-unitaries.

This leads us to conjecture that *all* two-qutrit 2-unitaries are LU equivalent to each other. From an exhaustive search, we find that the special subset of 72 possible 2-unitary permutations of size 9 are LU equivalent to each other. For local Hilbert-space dimension $d = 4$, we find that this still continues to hold: indeed, there are 6912 2-unitary permutations and we find that these can generated from any one of them by local permutations. Thus up to LU equivalence, we find that there is *only one* 2-unitary permutation in $d = 3$ and $d = 4$ and this implies that there is only one unique orthogonal Latin square (OLS) of size 3 and 4. Note that the connection between 2-unitary permutations and OLSs has been known for some time [60].

Although there is only one 2-unitary permutation up to LU equivalence, further below, we give an explicit example of a 2-unitary of size 16 that is not LU equivalent to any 2-unitary permutation of the same size. In other words, we give an explicit example of an AME state of four ququads that is not LU connected to an AME state of four ququads with minimal support. Minimal-support four-party AME states have d^2 nonvanishing coefficients in some product orthonormal basis, which is the smallest number possible [48]. These new examples of AME states can be used to construct new error-correcting codes, as has been done in Ref. [56], and can provide insights into the most general underlying combinatorial designs that 2-unitaries possess. For $d = 5$, we show that there are two LU-inequivalent 2-unitary permutations or, equivalently, two LU-inequivalent AME states of minimal support. This contradicts Conjecture 2 in Ref. [61], which implies that all four-party AME states of minimal support are LU equivalent for all local dimensions d.

A. Summary of principal results and structure of the paper

In view of the length of this paper, we summarize some of the main results here:

(1) Dynamical maps for generation of dual-unitary operators, given in Secs. III and IV:

  (a) It is shown in Proposition 1 that the map preserves local unitary equivalence.
  (b) An explicit form of the map for the two-qubit case is derived. This is used to show that all dual unitaries are period-2 points and, conversely, that all period-2 points are dual unitaries. It is shown that convergence of the map to dual unitaries is typically exponential.

(2) Quantum designs and new classes of 2-unitaries and AME states, set out in Secs. V–VII:

  (a) A necessary criterion for LU equivalence between bipartite unitary gates is proposed and is particularly useful for establishing inequivalence between 2-unitary operators and AME states.
  (b) An AME state of four qudits each of local dimension 4, AME$(4,4)$, is constructed such that it is not LU equivalent to any known AME state obtained from classical OLSs. It is likely to be the simplest genuine orthogonal quantum Latin-square construction.
  (c) For local dimensions $d = 3$ and $d = 4$, it is shown that there is only one LU class of AME states constructed from OLSs. However, we show that there is more than one such LU class for $d > 4$.

The paper is structured as follows. In Sec. II, the basic terminology used in the current work is defined. In Sec. III, the nonlinear iterative maps from which dual-unitary and 2-unitary operators are produced is described and their fixed-point structure is discussed. Stochastic generalizations are introduced and result in specially structured operators. In Sec. IV, the iterative map is studied in explicit forms for the case of qubits. Here, we analytically estimate

the power-law or exponential approach to dual-unitary operators. In Sec. V, combinatorial designs corresponding to dual-unitary operators are discussed. In Sec. VI, the question of the local unitary equivalence of 2-unitary operators is discussed, specially for the small cases of $d = 3$ and $d = 4$. In Sec. VII, permutations with small dimensions are studied in detail via their entangling powers and gate typicality. A classification of LU classes for dual-unitary and T-dual unitary permutation operators is given for $d = 2$ and $d = 3$. Finally, we conclude in Sec. VIII.

II. PRELIMINARIES AND DEFINITIONS

In this section, we mostly recall some relevant quantities and measures.

A. Operator entanglement and entangling power

Any operator $X \in \mathcal{B}(\mathcal{H}_d)$ is mapped to the state $|X\rangle \in \mathcal{H}_d \otimes \mathcal{H}_d$ as

$$|X\rangle := (X \otimes I)\,|\Phi\rangle\,, \tag{2}$$

where $\{|i\rangle\}_{i=1}^{d}$ is an orthonormal basis in $\mathcal{H}_d$ and $|\Phi\rangle := 1/\sqrt{d}\sum_{i=1}^{d}|ii\rangle$ is the generalized Bell state. A bipartite unitary operator $U = \sum_{ij}^{d^2}\alpha_{ij}\,e_i^A \otimes e_j^B \in \mathcal{B}(\mathcal{H}_d \otimes \mathcal{H}_d)$ is mapped to $|U\rangle = \sum_{ij}^{d^2}\alpha_{ij}\,|e_i\rangle_A \otimes |e_j\rangle_B \in \mathcal{H}_{d^2} \otimes \mathcal{H}_{d^2}$, where $e_i^{A,B}$ are a pair of operator bases in $\mathcal{B}(\mathcal{H}_d)$.

The entanglement of a unitary operator U is the entanglement of the state $|U\rangle = \sum_{j=1}^{d^2}\sqrt{\lambda_j}\,|X_j^A\rangle\,|Y_j^B\rangle$. The Schmidt decomposition of U is given by

$$U = \sum_{j=1}^{d^2}\sqrt{\lambda_j}X_j^A \otimes Y_j^B, \tag{3}$$

with $\mathrm{tr}X_j^{A\dagger}X_k^A = \mathrm{tr}Y_j^{B\dagger}Y_k^B = \delta_{jk}$, $\sum_{j=1}^{d^2}\lambda_j = d^2$. The *operator entanglement* of U is defined in terms of linear entropy as

$$E(U) = 1 - \frac{1}{d^4}\sum_{j=1}^{d^2}\lambda_j^2, \tag{4}$$

where $0 \le E(U) \le 1 - 1/d^2$.

Another related, but distinct, entanglement facet of a unitary operator U is its *entangling power*, $e_p(U)$. It is defined as the average entanglement produced due to its action on pure product states distributed according to the uniform Haar measure,

$$e_p(U) = C_d\overline{\mathcal{E}(U\,|\phi_1\rangle \otimes |\phi_2\rangle)}^{|\phi_1\rangle,|\phi_2\rangle}, \tag{5}$$

where $\mathcal{E}(\cdot)$ can be any entanglement measure and C_d is a constant scale factor. Considering $\mathcal{E}(\cdot)$ to be the linear entropy, the entangling power can be directly calculated using operator entanglement [37] as follows. Let S be the SWAP operator such that

$$S\,|\phi_A\rangle\,|\phi_B\rangle = |\phi_B\rangle\,|\phi_A\rangle\,, \tag{6}$$

for all $|\phi_A\rangle \in \mathcal{H}_d$, $|\phi_B\rangle \in \mathcal{H}_d$. We choose C_d such that the scaled entangling power $0 \le e_p(U) \le 1$ is given by

$$e_p(U) = \frac{1}{E(S)}[E(U) + E(US) - E(S)], \tag{7}$$

where $E(S) = 1 - 1/d^2$.

Note that the swap operator is such that it has the maximum possible operator entanglement; however, the entangling power $e_p(S) = 0$. For any operator U, $e_p(U) = e_p(US) = e_p(SU)$. The so-called gate typicality $g_t(U)$ [62] distinguishes these and is defined as

$$g_t(U) = \frac{1}{2E(S)}[E(U) - E(US) + E(S)]. \tag{8}$$

It also ranges from 0 to 1, with $g_t(S) = 1$, and it vanishes for all local gates.

B. Matrix reshaping

A bipartite unitary operator U on $\mathcal{H}^d \otimes \mathcal{H}^d$ can be expanded in the product basis as

$$U = \sum_{i\alpha j\,\beta}\langle i\alpha|U|j\,\beta\rangle\,|i\alpha\rangle\langle j\,\beta|\,. \tag{9}$$

There are four basic matrix rearrangements of U that we use in this work:

(1) Realignment operations:

$$R_1 : \langle i\alpha|U|j\,\beta\rangle = \langle\beta\alpha|U^{R_1}|ji\rangle, \tag{10}$$

$$R_2 : \langle i\alpha|U|j\,\beta\rangle = \langle ij\,|U^{R_2}|\alpha\beta\rangle. \tag{11}$$

(2) Partial-transpose operations:

$$\Gamma_1 : \langle i\alpha|U|j\,\beta\rangle = \langle j\,\alpha|U^{\Gamma_1}|i\beta\rangle, \tag{12}$$

$$\Gamma_2 : \langle i\alpha|U|j\,\beta\rangle = \langle i\beta|U^{\Gamma_2}|j\,\alpha\rangle. \tag{13}$$

The relation between entanglement and matrix reshapings becomes clear on considering the state $|U\rangle$ as now a four-party state $|\psi\rangle \in \mathcal{H}_d \otimes \mathcal{H}_d \otimes \mathcal{H}_d \otimes \mathcal{H}_d$:

$$|\psi\rangle_{ABCD} = (U_{AB} \otimes I_{CD})\,|\Phi\rangle_{AC}\,|\Phi\rangle_{BD}\,, \tag{14}$$

where $|\Phi\rangle = 1/\sqrt{d}\sum_i^d|ii\rangle$ is the generalized Bell state. The reduced states corresponding to the three possible

partitions $AB|CD$, $AC|BD$, and $AD|BC$ are given by

$$\rho_{AB} = \frac{1}{d^2} UU^\dagger,\ \rho_{AC} = \frac{1}{d^2} U^{R_2} U^{R_2\dagger},\ \rho_{AD} = \frac{1}{d^2} U^{\Gamma_2} U^{\Gamma_2\dagger}. \tag{15}$$

Using $(X \otimes Y)^{R_2} = |X\rangle\langle Y^*|$, where the asterisk ("*") refers to complex conjugation in the computational basis, it is easy to see that $U^{R_2} U^{R_2\dagger} = \sum_1^{d^2} \lambda_j |X_j\rangle\langle X_j|$. The Schmidt values λ_j are the singular values of U^{R_2} (which are the same as the singular values of U^{R_1}). The operator entanglement $E(U)$ can be interpreted as the linear entropy of entanglement of the bipartition $AC|BD$ and can be expressed in terms of U^R as

$$E(U) = 1 - \frac{1}{d^4} \mathrm{Tr}(U^R U^{R\dagger})^2. \tag{16}$$

Similarly, the operator entanglement $E(US)$ is the linear entropy of the bipartition $AD|BC$ and is

$$E(US) = 1 - \frac{1}{d^4} \mathrm{Tr}(U^\Gamma U^{\Gamma\dagger})^2. \tag{17}$$

Whenever the subscripts on R and Γ are dropped, they can refer equally to either of the two operations. Note that the singular values of U^R and U^Γ are all local unitary invariants (LUIs).

We recall definitions of some special families of unitary operators and also introduce some new families of unitary operators.

Definition 1: (dual unitary [17]). If the realigned matrix U^R of unitary operator U is also unitary, then U is called a dual unitary.

Definition 2: (T-dual unitary [50]). If the partial-transposed matrix U^Γ of a unitary operator U is also unitary, then U is called a T-dual unitary.

Definition 3: (2-unitary [48]). A unitary U for which both U^R and U^Γ are also unitary is called a 2-unitary.

Definition 4: (self-dual unitary). A unitary operator U for which $U^R = U$ is called a self-dual unitary.

Note that for a 2-unitary, $E(U) = E(US) = E(S) = 1 - 1/d^2$ are maximized and thus, from Eq. (7), $e_p(U) = 1$, the maximum possible value. Thus the corresponding four-party state given by Eq. (14) is maximally entangled along all three bipartitions and is an absolutely maximally entangled state of four qudits: AME$(4, d)$.

In the mathematics literature, the class of unitary operators that remain unitary under "block-transpose" have been studied since 1989 [63–69]. Referred to as biunitaries, they are dual unitary up to multiplication by SWAP and they are the result of the Γ_1 operation above. However, the term "biunitary" seems to be used interchangeably for both dual and T-dual-unitary operators and subsequently no special studies of 2-unitaries that are both dual and T-dual seem to exist.

T-dual and dual unitaries have very different entanglement properties, as reflected in their two most prominent representatives: the identity and the SWAP gate. However, they are related in the sense that every T-dual unitary U has a dual partner US (or SU). Note that if U is 2-unitary, so also are U^R and U^Γ. For example, the realignment of U^R is U itself, while $(U^R)^\Gamma = U^\Gamma S$, which is evidently unitary given that U is 2-unitary.

III. DUAL-UNITARY AND 2-UNITARY OPERATORS FROM NONLINEAR ITERATIVE MAPS

Complete parametrization of dual-unitary operators for arbitrary local Hilbert-space dimension d is not known in general except in the two-qubit case [17]. Several (incomplete) analytic constructions of families of dual-unitary operators have been proposed based on complex Hadamard matrices [70] and on diagonal [54] and block-diagonal unitary matrices [50]. Here, we briefly review the nonlinear maps introduced in Ref. [47] to generate unitary operators that are arbitrarily close to dual unitaries.

A. Dynamical map for dual unitaries

The following map is defined on the space of bipartite unitary operators:

$$\mathcal{M}_R : \mathcal{U}(d^2) \longrightarrow \mathcal{U}(d^2).$$

One complete action of $\mathcal{M}_R$ on a seed unitary U_0 consists of the following two steps:

(i) *Linear part*: realignment of U_0: $U_0 \xrightarrow{R} U_0^R$
(ii) *Nonlinear part*: projection of U_0^R to the nearest unitary matrix U_1 given by its polar decomposition (PD) [71,72]; $U_0^R = U_1 \sqrt{U_0^{R\,\dagger} U_0^R}$

Note that U_0^R must be of full rank for the map to be well defined, as the polar decomposition of rank-deficient matrices is not uniquely defined. We write one complete action of the map on U_0 as

$$\mathcal{M}_R[U_0] := U_1.$$

After n iterations,

$$\underbrace{\mathcal{M}_R \circ \mathcal{M}_R \circ \cdots \circ \mathcal{M}_R}_{n \text{ times}}[U_0] := \mathcal{M}_R^n[U_0] = U_n.$$

For arbitrary seeds, the map has been observed to almost certainly converge to dual unitaries [47] and this is made plausible by the following observations on the fixed points of the map $\mathcal{M}_R$.

An important property of the map is that *it preserves the local orbit* of seed unitary U_0 in the following sense.

Proposition 1:

$$\text{If } U_0' \overset{LU}{\sim} U_0, \text{ then } U_1' = \mathcal{M}_R[U_0'] \overset{LU}{\sim} U_1 = \mathcal{M}_R[U_0]. \tag{18}$$

Proof. We start from the identity [50]

$$\begin{aligned} U_0'^R &= [(u_1 \otimes u_2) U_0 (v_1 \otimes v_2)]^R \\ &= (u_1 \otimes v_1^T) U_0^R (u_2^T \otimes v_2), \end{aligned} \tag{19}$$

where T is the usual transpose. Using the polar decomposition of U_0^R, we obtain

$$\begin{aligned} U_0'^R &= (u_1 \otimes v_1^T) U_1 \sqrt{U_0^{R\,\dagger} U_0^R} (u_2^T \otimes v_2) \\ &= (u_1 \otimes v_1^T) U_1 (u_2^T \otimes v_2) \sqrt{U_0'^{R\,\dagger} U_0'^R} \\ &\equiv U_1' \sqrt{U_0'^{R\,\dagger} U_0'^R}. \end{aligned} \tag{20}$$

Explicitly,

$$\mathcal{M}_R[U_0'] = (u_1 \otimes v_1^T) \mathcal{M}_R[U_0] (u_2^T \otimes v_2). \tag{21}$$

■

Thus the changes in the operator entanglement under the $\mathcal{M}_R$ map are unaffected by local unitary operations.

Analogous to the $\mathcal{M}_R$ map for dual unitaries, one can define a $\mathcal{M}_\Gamma$ map to generate T-dual-unitary operators. The action of $\mathcal{M}_\Gamma$ on U_0 is defined as $\mathcal{M}_\Gamma[U_0] := U_1$, where U_1 is the closest unitary to U_0^Γ given by its polar decomposition. Such an algorithm has been independently studied in Ref. [73] to generate a special class of randomly structured bipartite unitary operators.

1. Dual unitaries as fixed points

The action of the map on a dual unitary U is

$$\mathcal{M}_R[\mathsf{U}] = \mathsf{U}^R,$$

as U^R is also unitary. As the realignment operation is an involution, $(X^R)^R = X$, it follows that $\mathcal{M}_R[\mathsf{U}^R] = \mathsf{U}$ and

$$\mathcal{M}_R^2[\mathsf{U}] = \mathsf{U}, \tag{22}$$

i.e., dual unitaries are period-2 fixed points of the map. Note that self-dual unitaries ($\mathsf{U}^R = \mathsf{U}$) are fixed points of the $\mathcal{M}_R$ map itself.

For the two-qubit case ($d^2 = 4$), we prove that dual unitaries are the *only* fixed points of the $\mathcal{M}_R^2$ map or, equivalently, the period-2 orbits of $\mathcal{M}_R$. However, for the two-qutrit case ($d^2 = 9$), there are fixed points of the $\mathcal{M}_R^2$ map other than dual unitaries (for an explicit example, see Appendix E). In this case, $U_0^R = U_1 \sqrt{U_0^{R\,\dagger} U_0^R}$, $U_1^R = U_0 \sqrt{U_1^{R\,\dagger} U_1^R}$ and the pair U_0 and U_1 conspire such that each one is the nearest unitary to the realignment of the other. Generic seeds are not of this kind; nor do they seem to end up in such pairs.

For $d^2 > 9$, we are unable to find such nondual fixed points. The reason why the map does not converge to such fixed points is because of large dimensionality: a random sampling of seed unitaries over the corresponding unitary group $\mathcal{U}(d^2)$ with $(d^2 - 1)$ parameters is unable to find appropriate seed unitaries that lead to such fixed points. One might also expect higher-order fixed points of the map, which makes the map a novel dynamical system in its own right, but for the purposes of this work we do not focus on such directions.

B. Dynamical map for 2-unitaries

The set of 2-unitary operators is a common intersection of dual and T-dual unitaries. In order to generate 2-unitary operators a slightly modified map, $\mathcal{M}_{\Gamma R}$ is used by also incorporating the partial-transpose operation. Schematically, the action of the map on seed unitary U_0 is

$$\mathcal{M}_{\Gamma R}: \; U_0 \xrightarrow{R} U_0^R \xrightarrow{\Gamma} \left(U_0^R\right)^\Gamma := U_0^{\Gamma R} \xrightarrow{\text{PD}} U_1. \tag{23}$$

It has been pointed out previously that sampling U_0 from the circular unitary ensemble (CUE), for small local dimensions ($d^2 = 9,\ 16$), $U_n = \mathcal{M}_{\Gamma R}^n[U_0]$ is arbitrarily close to being 2-unitary, with a significant probability; around 95% for $d^2 = 9$ and 20% for $d^2 = 16$ [47]. To generate 2-unitary operators in larger dimensions, one may need to start with an appropriate initial seed unitary, not just sampled from the CUE. This has been done in Ref. [56] to generate a 2-unitary of order 36, which has settled the long-standing problem of the existence of absolutely maximally entangled states of four parties in local dimensions six.

The search for 2-unitaries in the unitary group $\mathcal{U}(d^2)$ with d^4 parameters can be viewed as an optimization problem for maximizing the entangling power in a high-dimensional space with a complex landscape. Random seeds can get attracted to the many local extrema, which are typically saddles. This makes the search to find global extrema increasingly hard in higher dimensions. A glimpse of the difficulties involved is discussed in Ref. [74], where details about Hessians of the entangling power and especially its maximization in $d = 6$ are presented.

1. 2-unitaries as fixed points

An action of the $\mathcal{M}_{\Gamma R}$ map on a 2-unitary U is given by

$$\mathcal{M}_{\Gamma R}[\mathsf{U}] = \mathsf{U}^{\Gamma R},$$

as $\mathsf{U}^{\Gamma R} := \left(\mathsf{U}^{R}\right)^{\Gamma} = U^{\Gamma} S$ is also unitary. The combined rearrangement ΓR is not an involution like R or Γ but is equivalent to the identity operation when composed thrice. Note that the ΓR operation on the set of four symbols that label the indices of the product-basis states is $\{1,2,3,4\} \xrightarrow{R} \{1,3,2,4\} \xrightarrow{\Gamma} \{1,4,2,3\}$. Thus, iterating ΓR thrice results in

$$\{1,2,3,4\} \xrightarrow{\Gamma R} \{1,4,2,3\} \xrightarrow{\Gamma R} \{1,3,4,2\} \xrightarrow{\Gamma R} \{1,2,3,4\}\,.$$

Therefore, 2-unitaries are period-3 fixed points of the $\mathcal{M}_{\Gamma R}$ map:

$$\mathcal{M}^{3}_{\Gamma R}[\mathsf{U}] = \mathsf{U}. \tag{24}$$

C. Structured dual unitaries from stochastic maps

Analytic constructions of dual unitaries are obtained by multiplying T-dual unitaries with the swap S. The families of T-dual-unitary operators that have been analytically constructed so far mostly have a block-diagonal structure or are permutations (which can also be block diagonal) [50,75]. Dual-unitary permutations preserve dual unitarity under multiplication (both left as well as right) by arbitrary diagonal unitaries [50]. We refer to this property of dual-unitary permutations as an enphasing symmetry and it is a kind of gauge freedom enjoyed by these matrices. This symmetry is also present in the uniform block-diagonal constructions. In general, the iterative algorithms discussed above do not lead to dual unitaries with this symmetry. In these cases, no special structure of dual is usually evident, as illustrated in Fig. 1.

In this section, we demonstrate that modified algorithms can be defined that are capable of resulting in dual and 2-unitaries with block-diagonal structures or enphased permutations and hence afford some degree of control or design. This is achieved by incorporating in the algorithm random diagonal unitaries that preserve the dual-unitary property of structured matrices.

One such algorithm $\mathbb{M}_R$, which converges to dual unitaries with the enphasing symmetry, is defined as

$$\mathbb{M}_R:\ U_0 \xrightarrow{R} U_0^R \xrightarrow{\text{PD}} U_1' \to U_1 = D_1\, U_1'\, D_2, \tag{25}$$

where D_1 and D_2 are diagonal unitaries with random phases. Note that the map is no longer deterministic, as U_0 does not uniquely determine U_1. The map converges (in all cases that we have encountered for $d = 2$, $d = 3$, and $d = 4$) to dual unitaries that remain dual unitary upon multiplication by arbitrary diagonal unitaries.

Starting from a random-seed unitary U_0, the map converges to dual unitaries with different block structures as shown in Fig. 2 for $d^2 = 9$. For the sake of convenience, we show the nonzero elements of the corresponding T-dual unitary to the dual unitary obtained from the map. It is known that a block-diagonal unitary of size d^2 is T dual if the size of each block is a multiple of d [50]. The map indeed yields T-dual unitaries that are block diagonal and the size of each block is a multiple of d, as shown in Fig. 2 for $d^2 = 9$. The resulting dual unitaries are of the following form (up to multiplication by S):

(i) $U = \oplus_{i=1}^{3} u_i,\ u_i \in \mathcal{U}(3)$
(ii) $U = u_1 \oplus u_2,\ u_1 \in \mathcal{U}(6),\ u_2 \in \mathcal{U}(3)$

Due to their peculiar structure, these dual unitaries remain dual unitary under multiplication by random diagonal unitaries. This is easy to see for the uniform block case as compared to the nonuniform case in Fig. 2. In the nonuniform case, the 6×6 block cannot be replaced by an arbitrary unitary matrix. In fact, the 6×6 unitary matrix acting on $\mathcal{C}^2 \otimes \mathcal{C}^3$ should satisfy T-dual unitarity [50]. If we require in addition that the duality (or, equivalently, T duality) is preserved under multiplication by diagonal

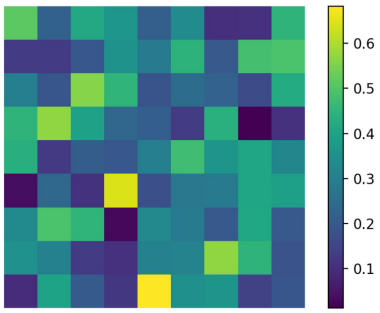

FIG. 1. The action of the $\mathcal{M}_R$ map, 1000 times, on a random-seed unitary of size $d^2 = 9$ results in an approximate dual unitary that typically has all d^4 entries nonzero. The absolute values of the matrix elements in one such instance are shown.

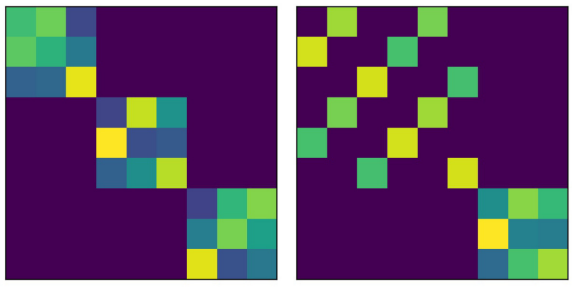

FIG. 2. Structured T-dual unitaries obtained using the $\mathbb{M}_R$ map for $d = 3$. Left: a T-dual unitary consisting of three blocks (unitary matrices) of size 3. Right: a T-dual unitary with a 6×6 block and a 3×3 block.

unitaries, a subset is picked, an example being shown in Fig. 2. Note the peculiar structure of the 6×6 block in the nonuniform case. It consists of three 2×2 unitary matrices arranged in such a way that multiplication by arbitrary diagonal unitaries preserves T duality.

We check that similar structured matrices are obtained for $d = 4$ and $d = 5$. For $d^2 = 16$, the map yields dual unitaries that are of the following forms (up to multiplication by S):

(i) $U = \oplus_{i=1}^{4} u_i$, $u_i \in \mathcal{U}(4)$
(ii) $U = \oplus_{i=1}^{2} u_i$, $u_i \in \mathcal{U}(8)$
(iii) $U = \oplus_{i=1}^{2} u_i$, $u_1 \in \mathcal{U}(4)$, $u_2 \in \mathcal{U}(12)$

These block structures are compatible with the analytical constructions of dual-unitary operators based on block-diagonal unitaries.

To obtain structured 2-unitaries, we define $\mathbb{M}_{\Gamma R}$ map as follows:

$$U_0 \xrightarrow{R} U_0^R \xrightarrow{\Gamma} \left(U_0^R\right)^\Gamma := U_0^{\Gamma R} \xrightarrow{\text{PD}} U_1' \to U_1 = D_1\, U_1'\, D_2. \tag{26}$$

For $d^2 = 9$, it is observed that for a random-seed unitary, if the map converges to 2-unitary then it is a 2-unitary permutation matrix up to multiplication by diagonal unitaries, as shown in Fig. 3. There is only one nonzero element in each row, positioned in such a way that the whole arrangement of nonzero entries in a 2-unitary permutation matrix is directly related to OLSs, which we elaborate in the following sections. The map is not as efficient as its deterministic counterpart $\mathcal{M}_{\Gamma R}$ in yielding 2-unitaries from random-seed unitaries. However, it demonstrates that one can obtain structured 2-unitary operators of desired symmetry and it can be used to gain insights into the most general constructions of such special unitary operators, We observe that multiplying at each step of the map with random but structured unitaries other than diagonal unitaries can also yield structured dual matrices, provided that duality is preserved under such operations.

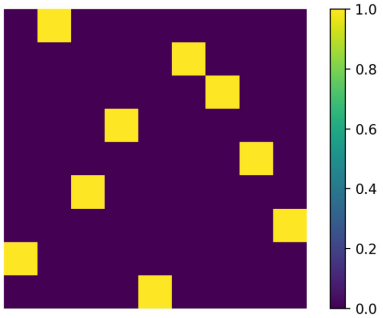

FIG. 3. The action of the $\mathbb{M}_{\Gamma R}$ map on a random-seed unitary of order 9. The map converges to 2-unitary permutation matrix (up to phases). The only nonzero element in each row or column is shown by a yellow square.

IV. DYNAMICAL MAP IN THE TWO-QUBIT CASE

The $\mathcal{M}_R$ map is now studied explicitly and analytically in the case of two-qubit unitary operators. The nonlocal part of the operators is well known in this case. As the map has been shown to be covariant under local unitary transformations [see Eq. (18)], it is sufficient to consider its action on the nonlocal part. The subset of dual-unitary matrices is known explicitly in this case and we can calculate the rate at which arbitrary seeds approach the dual set. We find that those that approach the SWAP gate S do so algebraically slowly, while generically the approach is exponential.

Any unitary operator in $\mathcal{U}(4)$ can be written as $(u_1 \otimes u_2)U(v_1 \otimes v_2)$, where u_i and v_i are single-qubit unitaries in $\mathcal{U}(2)$ and

$$U = \exp\left[-i \sum_{k=1}^{3} c_k\, (\sigma_k \otimes \sigma_k)\right]. \tag{27}$$

Here, the σ_k are Pauli matrices, the $c_k \in \mathbb{R}$ are *Cartan coefficients*, and U is the nonlocal part of the canonical Cartan form [76–78]. The so-called "Weyl chamber" [78] is a tetrahedron formed by considering the subset of c_k values:

$$0 \le |c_3| \le c_2 \le c_1 \le \frac{\pi}{4}. \tag{28}$$

The c_k values in the Weyl chamber that uniquely identify local unitarily inequivalent gates are also termed as the information content of the gate [79]. Below, we simply refer to the nonlocal part of U as the Cartan form. For two-qubit dual unitaries [17],

$$c_1 = c_2 = \frac{\pi}{4},\ c_3 \in \left[0, \frac{\pi}{4}\right], \tag{29}$$

and provides the complete parametrization of the nonlocal part. An equivalent parametrization is not known in higher dimensions.

A. $\mathcal{M}_R$ map in the Weyl chamber

While the map has been defined on general unitary matrices, the overall phase has no impact on entanglement and the map can be defined as an action on $\mathcal{SU}(4)$, with $\det(U) = 1$, to itself by removing the phase at each step. This turns out to be very useful for the qubit case.

Consider a seed unitary in Cartan form as

$$U_0 = \exp\left[-i\sum_{k=1}^{3} c_k^{(0)}\,(\sigma_k \otimes \sigma_k)\right] = \begin{pmatrix} e^{-ic_3^{(0)}} c_-^{(0)} & 0 & 0 & -ie^{-ic_3^{(0)}} s_-^{(0)} \\ 0 & e^{ic_3^{(0)}} c_+^{(0)} & -ie^{ic_3^{(0)}} s_+^{(0)} & 0 \\ 0 & -ie^{ic_3^{(0)}} s_+^{(0)} & e^{ic_3^{(0)}} c_+^{(0)} & 0 \\ -ie^{-ic_3^{(0)}} s_-^{(0)} & 0 & 0 & e^{-ic_3^{(0)}} c_-^{(0)} \end{pmatrix}, \tag{30}$$

where

$$c_\pm^{(n)} = \cos(c_1^{(n)} \pm c_2^{(n)}),$$
$$s_\pm^{(n)} = \sin(c_1^{(n)} \pm c_2^{(n)}),\ n = 0, 1, \ldots. \tag{31}$$

Note that $U_0 \in \mathcal{SU}(4)$ and we would like the subsequent iterations to also satisfy this property: it also becomes easy to identify the Cartan coefficients c_i at every step. A crucial property of the map is that it preserves the matrix form of U_0 such that U_1 has exactly the same structure (see Appendix A).

Let

$$U_n = \begin{pmatrix} \alpha_n & 0 & 0 & \beta_n \\ 0 & \delta_n & \gamma_n & 0 \\ 0 & \gamma_n & \delta_n & 0 \\ \beta_n & 0 & 0 & \alpha_n \end{pmatrix} \in \mathcal{SU}(4)\,, \tag{32}$$

where

$$\alpha_n = e^{-ic_3^{(n)}} c_-^{(n)},\ \beta_n = -ie^{-ic_3^{(n)}} s_-^{(n)},$$
$$\gamma_n = -ie^{ic_3^{(n)}} s_+^{(n)},\ \delta_n = e^{ic_3^{(n)}} c_+^{(n)}. \tag{33}$$

The mapping between matrix elements of U_{n+1} and U_n is given by

$$\alpha_{n+1} = \frac{e^{-i\frac{\chi_{n+1}}{4}}}{2}\left[\frac{\alpha_n+\delta_n}{|\alpha_n+\delta_n|} + \frac{\alpha_n-\delta_n}{|\alpha_n-\delta_n|}\right]$$
$$\beta_{n+1} = \frac{e^{-i\frac{\chi_{n+1}}{4}}}{2}\left[\frac{\alpha_n+\delta_n}{|\alpha_n+\delta_n|} - \frac{\alpha_n-\delta_n}{|\alpha_n-\delta_n|}\right]$$
$$\gamma_{n+1} = \frac{e^{-i\frac{\chi_{n+1}}{4}}}{2}\left[\frac{\beta_n+\gamma_n}{|\beta_n+\gamma_n|} - \frac{\beta_n-\gamma_n}{|\beta_n-\gamma_n|}\right]$$
$$\delta_{n+1} = \frac{e^{-i\frac{\chi_{n+1}}{4}}}{2}\left[\frac{\beta_n+\gamma_n}{|\beta_n+\gamma_n|} + \frac{\beta_n-\gamma_n}{|\beta_n-\gamma_n|}\right], \tag{34}$$

where

$$\chi_{n+1} = \mathrm{Arg}[(\alpha_n^2 - \delta_n^2)(\beta_n^2 - \gamma_n^2)]. \tag{35}$$

The dynamical system is thus a four-dimensional complex map on the manifold $S^4 \times S^4$. There are constraints originating from the unitarity condition: $|\alpha_i|^2 + |\beta_i|^2 = 1$, $|\gamma_i|^2 + |\delta_i|^2 = 1$, $\mathrm{Re}(\alpha_i\beta_i^*) = 0$, and $\mathrm{Re}(\gamma_i\delta_i^*) = 0$, and the $\mathcal{SU}$ condition: $(\alpha_n^2 - \beta_n^2)(\delta_n^2 - \gamma_n^2) = 1$. The nonlinear nature of the map is clear, as the entries of the above transformation are themselves functions of other variables.

Rather than the high-dimensional complex map in Eq. (34), using Eq. (33) we obtain a three-dimensional (3D) real map in terms of the Cartan coefficients. Defining $\theta_\pm^{(n)} = \mathrm{Arg}(\alpha_n \pm \delta_n)$ and $\phi_\pm^{(n)} = \mathrm{Arg}(\beta_n \pm \gamma_n)$, the complex map in Eq. (34) simplifies to

$$c_1^{(n+1)} = \frac{1}{4}(-\theta_+^{(n)} + \theta_-^{(n)} - \phi_+^{(n)} + \phi_-^{(n)}),$$
$$c_2^{(n+1)} = \frac{1}{4}(\theta_+^{(n)} - \theta_-^{(n)} - \phi_+^{(n)} + \phi_-^{(n)}),$$
$$c_3^{(n+1)} = \frac{1}{4}(-\theta_+^{(n)} - \theta_-^{(n)} + \phi_+^{(n)} + \phi_-^{(n)}). \tag{36}$$

Numerically, it is observed that the Cartan coefficients of $U_{n+1} = \mathcal{M}_R[U_n]$ obtained from the above 3D map agree for all even n with those calculated using the numerical algorithm presented in Ref. [79,80] and also satisfy Eq. (28). However, for odd n, the $c_3^{(n)}$ values still agree but the $c_1^{(n+1)}$ and $c_2^{(n+1)}$ values differ from the numerical value by $\pi/2$. In order to obtain the desired Cartan coefficients satisfying Eq. (28) from the above 3D map, one needs to replace $c_2^{(n+1)}$ by $\pi/2 - c_2^{(n+1)}$ for all odd n.

Before we simplify the 3D map given by Eq. (36), we first prove the following two theorems.

Theorem 1: *For two-qubit gates of the form Eq. (27), self-dual unitaries ($U = U^R$) are the only fixed points of the $\mathcal{M}_R$ map.*

Theorem 2: *For two-qubit gates of the form Eq. (27), dual unitaries are the only fixed points of the $\mathcal{M}_R^2$ map, i.e., $\mathcal{M}_R^2[U_0] = U_0$ if and only if U_0 is dual unitary.*

Proofs of the above theorems are presented in Appendix B.

Consider a two-qubit seed unitary U_0 parametrized by the Cartan parameters $c_1^{(0)}$, $c_2^{(0)}$, and $c_3^{(0)}$. Under the $\mathcal{M}_R$ map, U_0 is mapped to U_1, which is parametrized by $c_1^{(1)}$,

$c_2^{(1)}$, and $c_3^{(1)}$. The $\mathcal{M}_R$ map can be viewed most economically as a 3D dynamical map on the Cartan parameters,

$$U_n \xrightarrow{\mathcal{M}_R} U_{n+1},$$
$$(c_1^{(n)}, c_2^{(n)}, c_3^{(n)}) \xrightarrow{\mathcal{M}_R} (c_1^{(n+1)}, c_2^{(n+1)}, c_3^{(n+1)}). \quad (37)$$

B. Deriving the map for special initial conditions

Although we are unable to derive explicit maps in terms of these parameters for general $c_i^{(0)}$, we are able to do so for special values. We show that these converge to the desired fixed points, $c_1^{(n\to\infty)} = \pi/4$, $c_2^{(n\to\infty)} = \pi/4$, and $c_3^{(n\to\infty)} \in [0, \pi/4]$, which comprise the set of dual-unitary operators. This is depicted in Fig. 4 for a few random realizations evolved under the map for $n = 10$ steps. For the general case, we argue why this happens and also derive the rate of the exponential approach.

1. XY family: Plane $c_3 = 0$

The first special case is when $c_3^{(0)} = 0$ and $0 < c_2^{(0)} \leq c_1^{(0)}$. In this case, using Eq. (34), we can see that a *single* application of the $\mathcal{M}_R$ map results in the following unitary:

$$U_1 = \begin{pmatrix} 1 & 0 & 0 & 0 \\ 0 & 0 & -i & 0 \\ 0 & -i & 0 & 0 \\ 0 & 0 & 0 & 1 \end{pmatrix},$$

with $\det(U_1) = \det(U_0) = 1$. Thus the map preserves the $\mathcal{SU}$ property of seed unitaries. The Cartan parameters for U_1 are $c_1^{(1)} = c_2^{(1)} = \pi/4$ and $c_3^{(1)} = 0$ and therefore U_1 is dual unitary. This gate is LU equivalent to the DCNOT gate

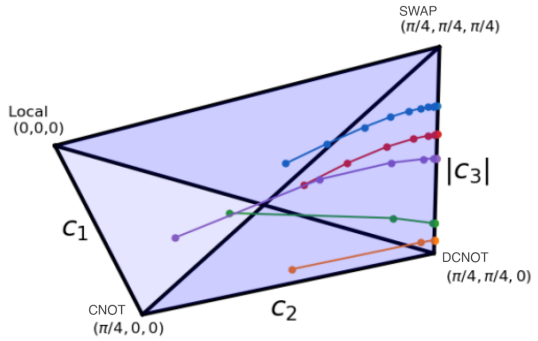

FIG. 4. Trajectories of five random realizations of two-qubit gates are shown inside the Weyl chamber under action of the map for $n = 10$ steps. The edge joining the SWAP gate and the DCNOT gate corresponds to dual unitaries to which the map converges.

[79], which is $S \times$ CNOT. Explicitly,

$$U_{\text{DCNOT}} = (H \otimes I)\, U_1\, (D_1 \otimes D_1\, H) = \begin{pmatrix} 1 & 0 & 0 & 0 \\ 0 & 0 & 0 & 1 \\ 0 & 1 & 0 & 0 \\ 0 & 0 & 1 & 0 \end{pmatrix}, \quad (38)$$

where $H = 1/\sqrt{2}\begin{pmatrix} 1 & 1 \\ 1 & -1 \end{pmatrix}$ is the Hadamard gate and $D_1 = P_{\pi/2} = \begin{pmatrix} 1 & 0 \\ 0 & i \end{pmatrix}$ is a phase gate.

Thus the entire interior of the base of the Weyl chamber, the $c_3 = 0$ plane, is mapped to the same dual-unitary gate U_1 in just one step and the rate at which it happens is infinite.

2. XXX family: $c_1 = c_2 = c_3$

Let $c_1 = c_2 = c_3 = c \in [0, \pi/4]$ in Eq. (27), the single-parameter family of unitary operators U:

$$U = \exp\left(-i\, c \sum_{i=1}^{3} \sigma_i \otimes \sigma_i\right). \quad (39)$$

This forms an edge of the Weyl chamber, the one that connects local unitaries to the SWAP gate S. Unitaries of this form are useful in many contexts, such as in the Trotterization of the integrable isotropic (XXX) Heisenberg Hamiltonian [81]. They are also, modulo phases, the fractional powers of the SWAP gate S as $U = \exp(-2\, i\, c\, S)$.

If we choose the seed unitary U_0 from this family with $c = c^{(0)}$, it follows from Eq. (33) that $\beta_0 = 0$. The action of the map on U_0 gives

$$U_1 = \begin{pmatrix} \alpha_1 & 0 & 0 & \beta_1 \\ 0 & 0 & \gamma_1 & 0 \\ 0 & \gamma_1 & 0 & 0 \\ \beta_1 & 0 & 0 & \alpha_1 \end{pmatrix}, \quad (40)$$

for which $\delta_1 = 0$. Note that U_1 is not exactly of the same form as U_0, for which $\beta_0 = 0$. In fact, for all even (odd) n, U_n is such that $\beta_n = 0$ ($\delta_n = 0$). For even n, $\beta_n = 0$ implies $c_1(n) = c_2(n)$ both being equal to $c_3^{(n)}$ and thus U_n belongs to the same family. However, for odd n, it is observed that although $c_2^{(n)} = c_3^{(n)} \leq \pi/4$, $c_1^{(1)} = \pi/2 - c_2^{(1)} \geq \pi/4$ and thus $c_1^{(1)}$ does not satisfy Eq. (28). Note that U_1 with Cartan coefficients $c_1^{(1)} = \pi/2 - c^{(1)}$ and $c_2^{(n)} = c_3^{(1)} = c^{(1)}$ is *not* LU equivalent to a gate with Cartan coefficients $c_1^{(n)} = c_2^{(n)} = c_3^{(1)} = c^{(1)}$, although in the part of the Weyl chamber to which we restrict our attention, they are the same points.

As a consequence of this, the 3D map given by Eq. (36) becomes a one-dimensional (1D) map.

Let $c^{(n)}$ be the Cartan coefficient parametrizing $U_n = \mathcal{M}_R^n[U_0]$ and

$$x_n = 1/\tan(2\,c^{(n)}). \tag{41}$$

The complications attendant on the ranges of c_i do not affect this variable. In terms of x_n (for a derivation, see Appendix C), the map takes a simple algebraic form,

$$x_{n+1} = \frac{2\,x_n}{1+\sqrt{4\,x_n^2+1}}. \tag{42}$$

The unique fixed point of the map is $x^* = 0$, corresponding to the SWAP gate, and the map is a contraction, as shown in Appendix C. Therefore, in the limit of large n, $x_n \to x^* = 0$. In this limit, Eq. (42) can be approximated as

$$x_{n+1} \approx x_n(1-x_n^2). \tag{43}$$

Thus, in the vicinity of the fixed point, the difference equation may be approximated by the differential equation $dx_n/dn = -x_n^3$. This is simple to solve and gives the large-n approximation to the map above as

$$x_n \approx 1/\sqrt{2n}. \tag{44}$$

3. SWAP-CNOT-DCNOT *face:* $c_1^{(0)} = \pi/4$

In this case, seed unitaries lie on the SWAP-CNOT-DCNOT face of the Weyl chamber with $c_1^{(0)} = \pi/4$. Under the action of the map, $c_1^{(n)} = \pi/4$ for all n and thus the corresponding map is two-dimensionally defined in terms of $c_2^{(n)}$ and $c_3^{(n)}$. An important property of the map observed in this case, which follows as $c_\pm = s_\mp$, is that the phase in Eq. (34), $\chi_{n+1} = 0$. This property is crucial for simplifying the map as shown below.

Defining $y_n = 1/\tan^2(2\,c_2^{(n)})$ and $z_n = 1/\tan^2(2\,c_3^{(n)})$, the corresponding two-dimensional (2D) map takes a purely algebraic form given by (for a derivation, see Appendix C)

$$\begin{aligned} y_{n+1} &= \frac{y_n}{1+z_n}, \\ z_{n+1} &= \frac{z_n}{1+y_n}. \end{aligned} \tag{45}$$

Although the above map has a symmetric form, due to the specific choice of Cartan parameters Eq. (28), the symmetry is broken and the fixed points are $y^* = 0$ (or $c_2^{(\infty)} = \pi/4$) and $z^* \in [0,\infty]$ (or $c_3^{(\infty)} \in [0,\pi/4]$), corresponding to the set of dual unitaries. This 2D map can be solved analytically by noting that

$$\Omega = \frac{1+y_{n+1}}{1+z_{n+1}} = \frac{1+y_n}{1+z_n} \tag{46}$$

is an invariant. Its value is determined by the initial conditions as

$$\Omega = \frac{1+y_0}{1+x_0} = \left(\frac{\sin(2\,c_3^{(0)})}{\sin(2\,c_2^{(0)})}\right)^2 < 1, \tag{47}$$

for $c_3^{(0)} < c_2^{(0)}$.

Using this to eliminate z_n, we have the 1D map

$$y_{n+1} = \Omega\frac{y_n}{1+y_n}, \tag{48}$$

which has the exact solution

$$y_n = \frac{\Omega^n\,y_0}{1+\left(\frac{1-\Omega^n}{1-\Omega}\right)\,y_0} \tag{49}$$

and implies that

$$z_n = \frac{z_0}{\Omega^n + \left(\frac{1-\Omega^n}{1-\Omega}\right)\,\Omega\,z_0}. \tag{50}$$

It follows from Eq. (49) that $y_\infty = 0$ and $z_\infty = 1/\Omega - 1$, respectively. Also, $c_3^{(\infty)}$, which parametrizes the dual unitary to which the map converges, can be written explicitly in terms of the initial pair $(c_2^{(0)}, c_3^{(0)})$ as

$$\begin{aligned} c_3^{(\infty)} &= \frac{1}{2}\arctan\left[\sqrt{\frac{\Omega}{1-\Omega}}\right] \\ &= \frac{1}{2}\arctan\left[\frac{\sin(2\,c_3^{(0)})}{\sqrt{\sin^2(2\,c_2^{(0)}) - \sin^2(2\,c_3^{(0)})}}\right]. \end{aligned} \tag{51}$$

Define $\Delta c_i^{(n)} = c_i^{(\infty)} - c_i^{(n)}$, where $c_1^{(\infty)} = c_2^{(\infty)} = \pi/4$, and $c_3^{(\infty)}$ is as above.

$$\begin{aligned} \Delta c_2^{(n)} &\sim |\sin 2\,c_3^{(\infty)}|^n, \\ \Delta c_3^{(n)} &\sim |\sin 2\,c_3^{(\infty)}|^{2\,n}. \end{aligned} \tag{52}$$

Note that $\Omega = \sin^2(2\,c_3^{(\infty)})$, governs the exponential approach to the duals. From the explicit and full solution in Eq. (49), it follows that we see below that these continue to hold for the general case as well.

The marginal case $\Omega = 1$ corresponds to seed unitaries on the SWAP-CNOT edge with $c_2^{(0)} = c_3^{(0)}$ and is dealt with separately below.

4. SWAP-CNOT *edge*

For these gates, $c_1^{(0)} = \pi/4$ and $c_2^{(0)} = c_3^{(0)}$ and is a special case of the face just discussed. In this case, the 2D map in Eq. (45) degenerates to a 1D map given by

$$y_{n+1} = \frac{y_n}{1 + y_n}, \tag{53}$$

with $\Omega = 1$. This map also can be solved analytically and the solution is given by

$$y_n = \frac{y_0}{\sqrt{n\, y_0^2 + 1}}. \tag{54}$$

The approach to the unique fixed point $y^* = 0$ is algebraic, in contrast to other gates on the SWAP-CNOT-DCNOT face, and goes as approximately $1/\sqrt{n}$. Thus the SWAP gate is approached slowly along both the edges that connect it in the Weyl chamber from the locals or from the CNOT gates. The other edge is the dual-unitary edge that is already a line of fixed points. In fact, the entire face of the Weyl chamber containing locals-SWAP-CNOT is mapped into itself and all initial conditions on this approach the dual-unitary SWAP gate algebraically. This face is characterized by two of the Cartan coefficients being equal, namely, $c_2^{(n)} = c_3^{(n)} \equiv c^{(n)}$. In the limit of large n, $\Delta c_1^{(n)} = \pi/4 - c_1^{(n)} \sim 1/n$ while $\Delta c_2^{(n)} = \Delta c_3^{(n)} = \pi/4 - c^{(n)} \sim 1/\sqrt{n}$.

5. *XXZ family:* $c_1 = c_2$

Let us now consider a family of two-qubit gates for which $c_1^{(0)} = c_2^{(0)} = c^{(0)} \in (0, \pi/4]$, and $c_3^{(0)} \le c^{(0)} \in [0, \pi/4]$. This restricts the seed unitaries to the face of the Weyl chamber that contains locals-SWAP-DCNOT. Under the action of the map, the unitaries remain on this face for even n and up to a local unitary transformation for odd n.

The map is two-dimensionally defined on $c_1^{(n)} = c_2^{(n)} = c^{(n)} \le \pi/4$ and $c_3^{(n)} \le c^{(n)}$ is given by

$$c^{(n+1)} = \frac{\pi}{4} - \frac{1}{4}\arctan \times \left\{ \frac{1}{2}\sin(2\, c_3^{(n)}) \left[\frac{1}{\tan^2(c^{(n)})} - \tan^2(c^{(n)}) \right] \right\}, \tag{55}$$

$$c_3^{(n+1)} = \frac{c_3^{(n)}}{2} + \frac{1}{4}\arctan \times \left\{ \frac{1}{2}\tan(2\, c_3^{(n)}) \left[\frac{1}{\tan^2(c^{(n)})} + \tan^2(c^{(n)}) \right] \right\}. \tag{56}$$

The fixed points consisting of $c^* = \pi/4$ and c_3^* can take any value in $[0, \pi/4]$, which is a line of fixed points corresponding to two-qubit dual unitaries. It is not hard to see that these are the only fixed points of the map.

The important information about the nature of the map can be obtained in the large-n limit, which is effectively a linear-stability analysis. For small $\Delta c^{(n)}$, Eq. (55) gives

$$\Delta c^{(n+1)} \approx \sin(2\, c_3^{(n)})\, \Delta c^{(n)}, \tag{57}$$

whereas Eq. (56) yields simply $c_3^{(n+1)} \approx c_3^{(n)}$ to first order in X_n, indicating that it can take any value, only determined by the initial condition. We denote this value as $c_3^* = c_3^{(\infty)}$. Thus the above equation is of the form $\Delta c^{(n+1)} = r \Delta c^{(n)}$, with $r = \sin(2\, c_3^{(\infty)})$, and we obtain the solution

$$\Delta c^{(n)} = e^{-n\xi}\, \Delta c^{(0)},\ \xi = |\ln r| = \left| \ln \sin(2\, c_3^{(\infty)}) \right|. \tag{58}$$

Therefore, the convergence to the respective fixed points, $c^* = \pi/4$ and $c_3^* = c_3^{(\infty)} \in [0, \pi/4]$, is also exponential, with the rate determined by the value $c_3^{(\infty)}$ as found in Eq. (52) for gates lying on the SWAP-CNOT-DCNOT face. This is shown qualitatively in Fig. 5. The rate $\xi = \infty$ when $c_3^{(\infty)} = 0$ and the unitaries converge to the DCNOT. This is consistent with the discussion in the XY discussion above, where it is shown that in this case just one step of the map is needed. The rate $\xi = 0$ is obtained for $c_3^{(\infty)} = \pi/4$, corresponding to asymptotic convergence to the SWAP gate. This is consistent with the discussion of the edge XXX above, where an algebraic approach is obtained.

For large n, the behavior of $\Delta c_3^{(n+1)} = c_3^{(\infty)} - c_3^{(n)}$ is found by analyzing Eq. (56), keeping the second-order

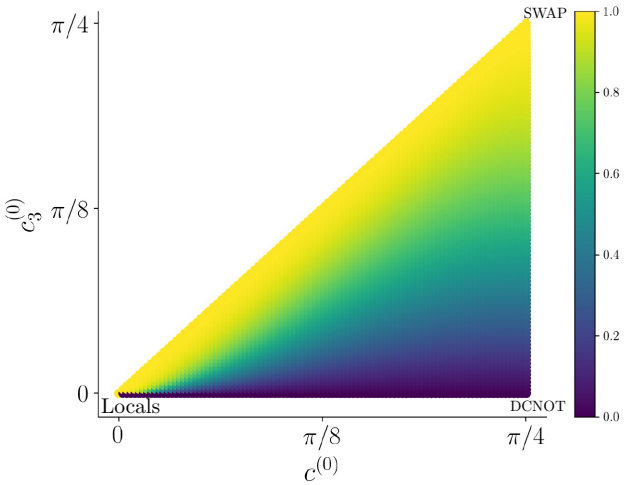

FIG. 5. Convergence in the XXZ case: the initial condition in the local-SWAP-DCNOT face. $r = \sin(2\, c_3^{(100)}) \approx \sin(2\, c_3^{(\infty)})$, which is related to the rate of convergence to a dual-unitary gate as $\xi = \ln r$, is plotted. Around 10^5 initial conditions $(c^{(0)}, c_3^{(0)})$ are taken and evolved for $n = 100$ times under the 2D map given in Eqs. (55)–(56). Initial conditions with $c_3^{(0)} = 0$, in the base of the triangle above, converge to the DCNOT gate at an infinite rate, while initial conditions with $c^{(0)} = c_3^{(0)} \in (0, \pi/4]$ converge to the SWAP gate at a vanishing rate, namely algebraically.

terms in $\Delta c^{(n)}$, and we obtain

$$\Delta c_3^{(n+1)} = \frac{1}{2}\sin(4c_3^{(\infty)})(\Delta c^{(n)})^2 = \frac{1}{2}\sin(4c_3^{(\infty)})e^{-n\xi_3}, \tag{59}$$

with $\xi_3 = 2\xi$, and hence the approach to $c_3^{(\infty)}$ is exponential at a rate that is *twice* that of the other Cartan parameters.

6. Generic initial conditions

Interestingly, the numerical results indicate that the exponential approach to $(\pi/4, \pi/4, c_3^{(\infty)})$ given in Eqs. (58) and (59) continues to hold for a generic initial condition inside the Weyl chamber. An illustration is displayed in Fig. 6 for the initial condition $(c_1^{(0)}, c_2^{(0)}, c_3^{(0)}) = (\pi/6, \pi/8, \pi/12)$. Under the map, it converges to a dual-unitary gate with $c_3^{\infty} \approx 0.443$. The rates ξ_1 and ξ_2 at which $\Delta c_1^{(n)} = \pi/4 - c_1^{(n)}$ and $\Delta c_2^{(n)} = \pi/4 - c_2^{(n)}$ approach 0 are almost the same, being given by $\xi = \left|\ln\sin(2\,c_3^{(\infty)})\right|$. The rate ξ_3 at which $\Delta c_3^{(n)} = c_3^{(\infty)} - c_3^{(n)} \to 0$ continues to be a very good approximation: $\xi_3 = 2\xi$. Initial conditions that converge to dual unitaries with large $c_3^{(\infty)}$ values, i.e., a small entangling power, take longer times. This is reflected in Fig. 4 for random realizations where gates that are closer to the SWAP gate take longer to reach the corresponding point on the dual-unitary edge.

We summarize the convergence of the map for different families in Table I. The slow algebraic approach holds for all initial conditions that approach the SWAP gate. In fact, we numerically verify that even for higher dimensions, $d > 2$, if the seed unitary is a fractional power of SWAP, they approach the dual-unitary SWAP gate algebraically as approximately $1/\sqrt{n}$.

It may be noted that a very different map on the Weyl chamber has been studied by looking at the powers of two-qubit gates in Ref. [82]. This map is ergodic on the Weyl chamber and is related to billiard dynamics in a tetrahedron, unlike the dissipative nature of the $\mathcal{M}_R$ map that we study.

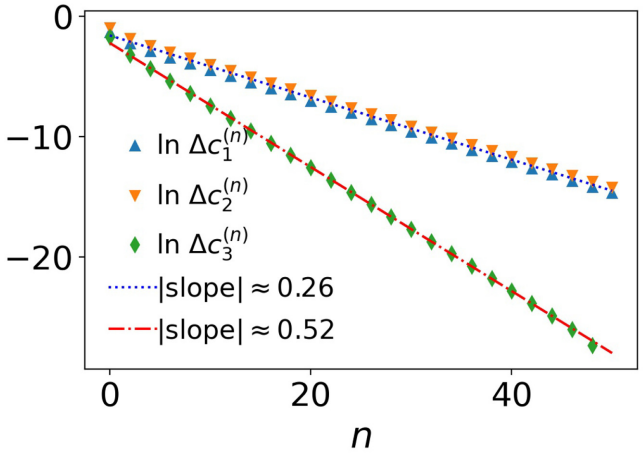

FIG. 6. Convergence for the initial condition inside the Weyl chamber: a seed unitary with $(c_1^{(0)}, c_2^{(0)}, c_3^{(0)}) = (\pi/6, \pi/8, \pi/12)$ is evolved under the map for $n = 50$ steps. Both quantities $\Delta c_1^{(n)} = \pi/4 - c_1^{(n)}$ and $\Delta c_2^{(n)} = \pi/4 - c_2^{(n)}$ decay exponentially with approximately the same rate $\xi = |\ln\sin(2c_3^{(\infty)})|$ determined by $c_3^{(\infty)} \approx 0.443$. The rate at which $\Delta c_3^{(n)} = c_3^{(\infty)} - c_3^{(n)} \to 0$ is almost twice that of $\Delta c_1^{(n)}$ or $\Delta c_2^{(n)}$. The numerically calculated slopes match with these values.

V. COMBINATORIAL DESIGNS CORRESPONDING TO DUAL-UNITARY OPERATORS

Tools developed in combinatorial mathematics have been very useful in constructing multipartite entangled states [48,59]. In Ref. [60], it has been shown that OLSs of order d can be used to construct 2-unitary permutation matrices of order d^2. Since 2-unitary operators belong to a subset of dual-unitary operators, we point to less restrictive combinatorial structures corresponding to general dual-unitary operators. In the case of dual-unitary permutations, such designs have been discussed earlier in Ref. [50], which we first summarize.

TABLE I. Convergence to dual unitaries for different two-qubit seed unitaries, parametrized by the Cartan coefficients $c_i^{(0)}$. In all cases, $c_1^{(\infty)} = c_2^{(\infty)} = \pi/4$ and $\Delta c_i = c_i^{(\infty)} - c_i^{(n)}$.

Cartan coefficients and Weyl-chamber location of seeds	Dual-unitary approached	Nature of convergence
Base, $c_3^{(0)} = 0$, $c_2^{(0)} > 0$	DCNOT, $c_3^{(1)} = c_3^{(\infty)} = 0$	Instantaneous, rate ∞
SWAP-local edge, $c_1^{(0)} = c_2^{(0)} = c_3^{(0)}$	SWAP	Algebraic, $\Delta c_i \sim 1/\sqrt{n}$
SWAP-local-CNOT face, $c_2^{(0)} = c_3^{(0)} \neq c_1^{(0)}$	$c_3^{(\infty)} = \pi/4$	Algebraic, Δc_3, $\Delta c_2 \sim 1/\sqrt{n}$, $\Delta c_1 \sim 1/n$
SWAP-local-DCNOT face, $c_1^{(0)} = c_2^{(0)} \neq c_3^{(0)}$	Generic	Exponential,
SWAP-CNOT-DCNOT face, $c_1^{(0)} = \pi/4$, $c_2^{(0)} \neq c_3^{(0)}$		$\Delta c_1, \Delta c_2 \sim \exp(-\xi\, n)$, $\Delta c_3 \sim \exp(-2\xi\, n)$
Interior, $c_1^{(0)} > c_2^{(0)} > c_3^{(0)}$	$c_3^{(\infty)} \neq 0,\ \pi/4$	$\xi = \lvert\ln\sin(2c_3^{(\infty)})\rvert$

A. Permutation matrices: Classical design

A permutation of d^2 symbols or elements from $[d] \times [d]$, $[d] = \{1, 2, \ldots, d\}$, is specified by the operator on computational product-basis states $|ij\rangle$ as

$$P\,|ij\rangle = |k_{ij}\, l_{ij}\rangle\,. \tag{60}$$

Thus, this can be written in terms of a pair of $d \times d$ matrices $K = (k_{ij})$ and $L = (l_{ij})$. In Ref. [50], it has been shown that for P to be dual unitary (T dual), the conditions on the K and L matrices are as follows:

(i) *Condition on K*: no element repeats along any *row* (*column*).
(ii) *Condition on L*: no element repeats along any *column* (*row*).

As an example, for $d = 2$, the dual-unitary SWAP gate permutes the basis states as

$$\begin{array}{|cc|}\hline 11 & 12 \\ 21 & 22 \\ \hline\end{array} \longrightarrow \begin{array}{|cc|}\hline 11 & 21 \\ 12 & 22 \\ \hline\end{array}, \tag{61}$$

with K and L given by

$$K = \begin{array}{|cc|}\hline 1 & 2 \\ \hline 1 & 2 \\ \hline\end{array},\quad L = \begin{array}{|c|c|}\hline 1 & 1 \\ \hline 2 & 2 \\ \hline\end{array}. \tag{62}$$

OLSs denoted OLS(d) [83] are examples of designs used to construct the 2-unitary operators [60]. A Latin square is a $d \times d$ array with d distinct elements such that every element appears exactly once in each column and in each row. Two Latin squares with elements s_{ij} and t_{ij} are orthogonal if the ordered pairs (s_{ij}, t_{ij}) are all distinct.

If K and L, defined above, are Latin squares, then the corresponding permutation matrix P is both dual unitary and T dual; hence it is 2-unitary. OLS(d) exists for all d except $d = 2$ and $d = 6$ [84]. Thus 2-unitary permutations exist for all d values except $d = 2$ and $d = 6$. An example of an OLS(3) is the following:

$$\begin{array}{|ccc|}\hline 1 & 2 & 3 \\ 3 & 1 & 2 \\ 2 & 3 & 1 \\ \hline\end{array} \cup \begin{array}{|ccc|}\hline 1 & 3 & 2 \\ 3 & 2 & 1 \\ 2 & 1 & 3 \\ \hline\end{array} = \begin{array}{|ccc|}\hline 11 & 23 & 32 \\ 33 & 12 & 21 \\ 22 & 31 & 13 \\ \hline\end{array}. \tag{63}$$

Note that all nine pairs from the set $\{1, 2, 3\} \times \{1, 2, 3\} = \{11, 12, \ldots, 32, 33\}$ are present.

For dual-unitary or T-dual permutations, K and L are not Latin squares in general. We define the *r-Latin square (c-Latin square)* as an arrangement of d symbols in a $d \times d$ array if it satisfies the conditions of a Latin square only along the rows (columns). Note that the usual Latin square is both r-Latin square as well as c-Latin square. Two such less constrained Latin squares are orthogonal if by superposing them all, the d^2 ordered pairs obtained are distinct. For dual-unitary permutations, K is r-Latin square and L is c-Latin square, while for T-dual permutations, K is c-Latin square and L is r-Latin square, which are restatements of the above conditions for duality (T duality).

B. General dual-unitary operators: Quantum design

Here, we discuss the underlying combinatorial structure of general dual-unitary operators. Consider a unitary operator $U \in \mathcal{B}(\mathcal{H}_d \otimes \mathcal{H}_d)$. Define

$$|\psi_{ij}\rangle = U\,|ij\rangle\,, \tag{64}$$

where $\{|ij\rangle\}_{i,j=1}^{d}$ is the computational basis in $\mathcal{H}_d \otimes \mathcal{H}_d$. The unitarity of U implies that the set of vectors $\{|\psi_{ij}\rangle\}_{i,j=1}^{d}$ also forms an orthonormal basis in $\mathcal{H}_d \otimes \mathcal{H}_d$.

Consider the $|\psi_{ij}\rangle$, which are of product form

$$|\psi_{ij}\rangle = |\alpha_{ij}\rangle \otimes |\beta_{ij}\rangle\,. \tag{65}$$

Analogous to K and L defined in the previous section for permutation operators, we arrange d^2 single-qudit states $|\alpha_{ij}\rangle$ and $|\beta_{ij}\rangle$ as follows:

$$\mathcal{K} = \begin{array}{|cccc|}\hline |\alpha_{11}\rangle & |\alpha_{12}\rangle & \cdots & |\alpha_{1d}\rangle \\ |\alpha_{21}\rangle & |\alpha_{22}\rangle & \cdots & |\alpha_{2d}\rangle \\ \vdots & \vdots & \vdots & \vdots \\ |\alpha_{d1}\rangle & |\alpha_{d2}\rangle & \cdots & |\alpha_{dd}\rangle \\ \hline\end{array}$$

$$\mathcal{L} = \begin{array}{|cccc|}\hline |\beta_{11}\rangle & |\beta_{12}\rangle & \cdots & |\beta_{1d}\rangle \\ |\beta_{21}\rangle & |\beta_{22}\rangle & \cdots & |\beta_{2d}\rangle \\ \vdots & \vdots & \vdots & \vdots \\ |\beta_{d1}\rangle & |\beta_{d2}\rangle & \cdots & |\beta_{dd}\rangle \\ \hline\end{array}. \tag{66}$$

The conditions for U to be dual unitary in terms of $\mathcal{K}$ and $\mathcal{L}$ are presented below.

Theorem 3: *If every row of $\mathcal{K}$ and every column of $\mathcal{L}$ forms an orthonormal basis in $\mathcal{H}_d$, then the unitary operator $U = \sum_{i,j=1}^{d} |\psi_{ij}\rangle\langle ij| = \sum_{i,j=1}^{d} |\alpha_{ij}\,\beta_{ij}\rangle\langle ij|$ is dual unitary.*

Proof. The orthonormality condition on the vectors in every row of $\mathcal{K}$ and every column of $\mathcal{L}$ implies that $\langle\alpha_{ij}|\alpha_{ij'}\rangle = \delta_{jj'}$, $\sum_{j=1}^{d} |\alpha_{ij}\rangle\langle\alpha_{ij}| = I_d$, $\forall\ i$ and $\langle\beta_{ij}|\beta_{i'j}\rangle = \delta_{ii'}$, $\sum_{i=1}^{d} |\beta_{ij}\rangle\langle\beta_{ij}| = I_d$, $\forall\ j$. Using these conditions, it follows that

$$\begin{aligned} U^R U^{R\dagger} &= \left(\sum_{i,j=1}^{d} |\alpha_{ij}\, i\rangle\, \langle\beta_{ij}\, j|\right)\left(\sum_{i',j'=1}^{d} |\beta_{i'j'}\, j'\rangle\, \langle\alpha_{i'j'}\, i'|\right), \\ &= \left(\sum_{j=1}^{d} |\alpha_{ij}\rangle\, \langle\alpha_{ij}|\right) \otimes \left(\sum_{i=1}^{d} |i\rangle\langle i|\right), \\ &= I_d \otimes I_d = I_{d^2}. \end{aligned}$$

It is similarly shown that $U^{R\dagger}U^{R} = I_{d^2}$ and hence unitary U is dual unitary. ■

The conditions on $\mathcal{K}$ and $\mathcal{L}$ for U to be dual unitary are generalizations of K and L corresponding to dual-unitary permutations. In K and L, the notion of symbols being *different* in a row or column is replaced by its quantum analog, the *orthogonality* of vectors (quantum states). In fact, such a generalization is known for Latin square and OLS referred as quantum Latin square (QLS) [85] and orthogonal quantum Latin square (OQLS) [59,86], respectively. A quantum Latin square is a $d \times d$ array of d-dimensional vectors such that each row and each column forms an orthonormal basis in $\mathcal{H}_d$. Two quantum Latin squares are orthogonal if, together, they form an orthonormal basis in $\mathcal{H}_d \otimes \mathcal{H}_d$. If $\mathcal{K}$ and $\mathcal{L}$ defined above are quantum Latin squares, then U is a 2-unitary operator [59].

The fact that there are no repetitions of symbols in a Latin square in any row or column translates into orthogonality of vectors in each row and column in the corresponding QLS. The "quantumness" and equivalence between quantum Latin squares has been defined in Ref. [87] in terms of the number of distinct basis vectors (up to phases), known as the *cardinality*. For QLSs constructed from classical Latin squares, simply by replacing the symbol k by a basis vector $|k\rangle$ in a d dimensional space, the cardinality is d and is said to be *classical*.

Quantum Latin squares with cardinality more than d cannot be obtained from classical Latin squares using unitary transformations of the basis vectors and are referred to as *genuinely quantum* [87]. Quantum Latin squares with cardinality equal to d^2, the maximum possible value, for general d and their relation to quantum sudoku are discussed in Refs. [87,88].

For dual-unitary or T-dual-unitary operators, $\mathcal{K}$ and $\mathcal{L}$ are not quantum Latin squares in general. We define the r-quantum Latin square (c-quantum Latin square) denoted by r-QLS (c-QLS) as a $d \times d$ array of d-dimensional vectors if it satisfies the conditions of a quantum Latin square only along the rows (columns). Note that the quantum Latin square is both r-QLS as well as c-QLS. For dual-unitary operators, $\mathcal{K}$ is r-QLS and $\mathcal{L}$ is c-QLS, while for T-dual operators, $\mathcal{K}$ is c-QLS and $\mathcal{L}$ is r-QLS.

Two such less constrained QLS are said to be orthogonal if, together, they form an orthonormal basis in $\mathcal{H}_d \otimes \mathcal{H}_d$. In analogy with cardinality of a quantum Latin square, we define the cardinality of $\mathcal{K}$ or $\mathcal{L}$ as the number of distinct basis vectors (up to phases) that they contain. An r-QLS or c-QLS of size d is *classical* if it contains d distinct basis vectors and *genuinely quantum* if it contains more than d distinct basis vectors. For dual-unitary permutations, the cardinality of $\mathcal{K}$ and $\mathcal{L}$ is always equal to d and thus they are classical. An example of a pair of genuine r-QLS and c-QLS of size 3 are, respectively,

$$\mathcal{K}: \begin{array}{|c|c|c|} \hline |1\rangle & |2\rangle & |3\rangle \\ \hline |1\rangle & |2\rangle & |3\rangle \\ \hline \frac{1}{\sqrt{2}}(|1\rangle + |2\rangle) & \frac{1}{\sqrt{2}}(|1\rangle - |2\rangle) & |3\rangle \\ \hline \end{array}, \tag{67}$$

$$\mathcal{L}: \begin{array}{|c|c|c|} \hline |1\rangle & -|1\rangle & \frac{1}{\sqrt{2}}(|1\rangle + |2\rangle) \\ \hline |2\rangle & |2\rangle & |3\rangle \\ \hline |3\rangle & |3\rangle & \frac{1}{\sqrt{2}}(|1\rangle - |2\rangle) \\ \hline \end{array}. \tag{68}$$

Note that both $\mathcal{K}$ (r-QLS) and $\mathcal{L}$ (c-QLS) contain five distinct basis vectors (quantum states), across two different orthonormal bases, and are thus genuinely quantum. Together, $\mathcal{K}$ and $\mathcal{L}$ form an orthonormal basis in $\mathcal{H}_3 \otimes \mathcal{H}_3$ arranged in a $d \times d$ array as

$$\begin{array}{|c|c|c|} \hline |1\rangle \otimes |1\rangle & -|2\rangle \otimes |1\rangle & |3\rangle \otimes \frac{1}{\sqrt{2}}(|1\rangle + |2\rangle) \\ \hline |1\rangle \otimes |2\rangle & |2\rangle \otimes |2\rangle & |3\rangle \otimes |3\rangle \\ \hline \frac{1}{\sqrt{2}}(|1\rangle + |2\rangle) \otimes |3\rangle & \frac{1}{\sqrt{2}}(|1\rangle - |2\rangle) \otimes |3\rangle & |3\rangle \otimes \frac{1}{\sqrt{2}}(|1\rangle - |2\rangle) \\ \hline \end{array}. \tag{69}$$

The dual-unitary gate corresponding to the above arrangement of size 9 is

$$U_9 = \begin{pmatrix} 1 & 0 & 0 & 0 & 0 & 0 & 0 & 0 & 0 \\ 0 & 0 & 0 & 1 & 0 & 0 & 0 & 0 & 0 \\ 0 & 0 & 0 & 0 & 0 & 0 & \frac{1}{\sqrt{2}} & \frac{1}{\sqrt{2}} & 0 \\ 0 & -1 & 0 & 0 & 0 & 0 & 0 & 0 & 0 \\ 0 & 0 & 0 & 0 & 1 & 0 & 0 & 0 & 0 \\ 0 & 0 & 0 & 0 & 0 & 0 & \frac{1}{\sqrt{2}} & -\frac{1}{\sqrt{2}} & 0 \\ 0 & 0 & \frac{1}{\sqrt{2}} & 0 & 0 & 0 & 0 & 0 & \frac{1}{\sqrt{2}} \\ 0 & 0 & \frac{1}{\sqrt{2}} & 0 & 0 & 0 & 0 & 0 & -\frac{1}{\sqrt{2}} \\ 0 & 0 & 0 & 0 & 0 & 1 & 0 & 0 & 0 \end{pmatrix}, \tag{70}$$

with $(e_p(U_9), g_t(U_9)) = (3/4, 5/8)$. This dual unitary is not locally equivalent to any dual-unitary permutation matrix (the corresponding $\mathcal{K}$ and $\mathcal{L}$ contain only three distinct vectors) with the same entangling power and gate typicality. We obtain the dual unitary U_9 using the $\mathcal{M}_R$ map (see Sec. III A). This is one of the nice properties of the map, in that it yields structured dual unitaries by choosing appropriate seed unitaries such as permutations. For $e_p(U) < 1$, it is relatively easier to construct dual unitaries that are LU inequivalent to dual-unitary permutations with the same entangling power. However, for $e_p(U) = 1$, i.e., 2-unitaries, this is not the case, as they satisfy additional constraints, which we discuss in the next section.

C. Combinatorial structures of known families of dual unitaries

1. Diagonal ensemble

Dual unitaries have one-to-one correspondence with T-dual-unitary operators, which are easier to construct. The simplest ensemble of T-dual unitaries one can think of is that of diagonal unitaries with arbitrary phases, denoted D_1. A d^2-parameter subset of dual unitaries can be obtained by (premultiplying or postmultiplying diagonal unitaries with the SWAP gate S [50,54]. It is easy to see that for dual unitaries of the form $U = D_1 S$ obtained from the diagonal ensemble,

$$U(|k\rangle \otimes |l\rangle) = D_1 S(|k\rangle \otimes |l\rangle) = \exp(i\,\theta_{lk})(|l\rangle \otimes |k\rangle). \tag{71}$$

Thus, the corresponding $\mathcal{K}$ and $\mathcal{L}$ are same as that of the SWAP gate (up to phases) and hence are classical.

2. Block-diagonal ensemble

A more general d^3-parameter family of dual-unitary gates, $U = D_d S$, can be obtained from block-diagonal unitaries [50,75,89], given by

$$D_d = \sum_{i=1}^{d} |i\rangle\langle i| \otimes u_i,\ u_i \in \mathcal{U}(d). \tag{72}$$

This is a controlled unitary from the first subsystem to the second. For this family of dual unitaries, the combinatorial structures are given by

$$\mathcal{K}: \begin{array}{|c|c|c|c|}\hline |1\rangle & |2\rangle & \cdots & |d\rangle \\ \hline |1\rangle & |2\rangle & \cdots & |d\rangle \\ \hline \vdots & \vdots & \vdots & \vdots \\ \hline |1\rangle & |2\rangle & \cdots & |d\rangle \\ \hline \end{array},$$

$$\mathcal{L}: \begin{array}{|c|c|c|c|}\hline u_1|1\rangle & u_2|1\rangle & \cdots & u_d|1\rangle \\ u_1|2\rangle & u_2|2\rangle & \cdots & u_d|2\rangle \\ \vdots & \vdots & \vdots & \vdots \\ u_1|d\rangle & u_2|d\rangle & \cdots & u_d|d\rangle \\ \hline \end{array}, \tag{73}$$

where the u_t values are related to the dual unitary $U = D_d S$ by Eq. (72). Note that the orthonormality along the columns in $\mathcal{L}$ is ensured by the identical unitary transformation of each basis vector. Although $\mathcal{K}$ contains only d distinct vectors and is classical, $\mathcal{L}$ contains in general d^2 (the maximum possible number) of distinct vectors and hence is genuinely quantum.

The quantum designs considered so far, such as the ones above, are mostly unentangled. Generalizations to entangled designs are needed to describe, for example, the recently found 2-unitary operator behind the AME(4, 6) state [56]. Although one can write necessary and sufficient conditions for U to be 2-unitary (see Appendix D), in terms of reduced-density matrices of bipartite states defined in Eq. (64), the orthogonality relations in the corresponding OQLS are harder to interpret than in OLS.

A unitary gate U on $\mathcal{H}_d \otimes \mathcal{H}_d$ is an *universal entangler* if $U(|\alpha_i\rangle \otimes |\beta_i\rangle)$ is *always* entangled for any choice of the product state $|\alpha_i\rangle \otimes |\beta_i\rangle$. It is known that universal entanglers do not exist for $d = 2$ and $d = 3$, i.e., there is no two-qubit or two-qutrit unitary gate that maps every product state to an entangled state [90]. It is easy to see that all columns of a universal entangler must be entangled; however, this condition is necessary but not sufficient [91]. Those dual-unitary and 2-unitary gates that are universal entanglers will have genuinely entangled quantum designs. Unfortunately, there are no known constructions of universal entanglers and the conditions under which they are obtained are not known.

VI. LOCAL UNITARY EQUIVALENCE OF 2-UNITARY OPERATORS

A. A necessary criterion

Given any two bipartite unitary operators U and U', as far as we know, there is no procedure to determine if they are LU equivalent, $U \overset{\text{LU}}{\sim} U'$, or not denoted by namely $U \overset{\text{LU}}{\sim} U'$ if Eq. (1) is satisfied for some local operators u_i and v_i. The problem is exacerbated for the case of 2-unitary operators, as the singular values of U^R and U^Γ, which are LUIs, are all equal and hence maximize the standard invariants such as $E(U)$ and $E(US)$.

Here, we propose a necessary criterion to investigate the LU equivalence between unitary operators based on the distributions of the entanglement they produce when applied on an ensemble of uniformly generated product states. The action of a bipartite unitary operator U on product states generically results in entangled states:

$$|\psi_{AB}\rangle = U(|\phi_A\rangle \otimes |\phi_B\rangle). \tag{74}$$

Let $\mathcal{E}(|\psi\rangle_{AB})$ be any measure of entanglement and let ϕ_A and ϕ_B be sampled from the Haar measure on the

subspaces. Then, the resulting distribution $p(x;U)$ of the entanglement is

$$p(x;U) = \int \delta\left(x - \mathcal{E}[U(|\phi_A\rangle \otimes |\phi_B\rangle)]\right) d\mu(\phi_A) d\mu(\phi_B). \tag{75}$$

It is clear that if U is left multiplied by local unitaries, $p(x;U)$ is unchanged, as entangled measures are invariant under such operations. If $U' = U(u_A \otimes u_B)$, then $p(x;U') = p(x;U)$, as $d\mu(u_A^\dagger |\phi_A\rangle) = d\mu(|\phi_A\rangle)$, which is a property of the Haar measure. Thus, if $U \overset{\text{LU}}{\sim} U'$, then $p(x;U') = p(x;U)$. Conversely, if $p(x;U') \neq p(x;U)$, this implies that $U \overset{\text{LU}}{\not\sim} U'$.

However, if the distributions are *indistinguishable*, i.e., $p(x;U') = p(x;U)$, then U and U' *may* or *may not* be LU equivalent. To see that the criterion is necessary but not sufficient, consider two LU-inequivalent operators U and $U' = US$, where S is the SWAP gate. Although U and U' are LU inequivalent, they generate identical entanglement distributions, $p(x;U) = p(x;U')$. Note that U and U' have the same entangling power, $e_p(U) = e_p(U')$, but have different gate typicalities, $g_t(U) \neq g_t(U')$, and are thus LU inequivalent.

We enlarge the local equivalence between U and U' to include multiplication by SWAP gates on either or both sides, denoted by $U' \overset{\text{LUS}}{\sim} U$ as

$$U' = (u_1 \otimes v_1)\, S^a\, U\, S^b\, (u_2 \otimes v_2), \tag{76}$$

where the u_i and v_i are single-qudit gates and a and b take the values 0 or 1. Any operator in the LUS equivalence class of U will produce the same entanglement distribution, $p(x;U)$.

B. 2-unitaries in $d = 3$

1. Permutations

The 2-unitary permutations of order d^2 maximize the entangling power and are in one-to-one correspondence with OLSs of size d; OLS(d) [60]. In general, 2-unitary operators are in one-to-one correspondence with AME states of four qudits [48]. Under this mapping, 2-unitary permutation matrices correspond to AME states with minimal support [48], i.e., these contain minimal possible terms equal to d^2 when written in the computational basis. A complete enumeration of all possible 2-unitary permutations of size d^2 boils down to the possible number of OLS(d), which is known for $d \leq 9$ (see A072377, Ref. [92]). For $d = 3$, there are 72 possible 2-unitary permutations of size 9. We find by a direct numerical exhaustive search over local permutation matrices of size 3 that *all* 72 possible 2-unitary permutations are LU equivalent. This observation leads to the following proposition.

Proposition 2: *There is only one LU class of 2-unitary permutations of order 9.*

We choose the following 2-unitary permutation as a representative of the LU-equivalent class of 2-unitary permutations of order 9:

$$P_9 = \left(\begin{array}{ccc|ccc|ccc} 1 & . & . & . & . & . & . & . & . \\ . & . & . & . & 1 & . & . & . & . \\ . & . & . & . & . & . & . & . & 1 \\ \hline . & . & . & . & . & 1 & . & . & . \\ . & . & . & . & . & . & 1 & . & . \\ . & 1 & . & . & . & . & . & . & . \\ \hline . & . & . & . & . & . & . & 1 & . \\ . & . & 1 & . & . & . & . & . & . \\ . & . & . & 1 & . & . & . & . & . \end{array}\right). \tag{77}$$

An easy way to obtain all 72 possible 2-unitary permutations is by searching over $(3!)^4 = 1296$ local permutations p_i of size 3 in

$$P' = (p_1 \otimes p_2) P_9 (p_3 \otimes p_4). \tag{78}$$

Although this is not an efficient way, as each 2-unitary permutation is repeated 18 times, all $1296/18 = 72$ possible permutations can be obtained.

An equivalent statement in terms of LU equivalence of AME$(4,3)$ states with minimal support is known (see Ref. [61]). An AME$(4,3)$ state with minimal support considered in Ref. [61] contains arbitrary phases and is equivalent to an enphased 2-unitary permutation, i.e., a 2-unitary permutation multiplied by a diagonal unitary. It is a special property of 2-unitary permutations that these remain 2-unitary upon multiplication by diagonal unitaries, with arbitrary phases, owing to their special combinatorial structure. Indeed, one can show that in $d = 3$, all enphased permutations are LU equivalent to P_9. Local dimension $d = 3$ is special in the sense that number of phases, $d^2 - 1 = 8$, exactly matches the number of phases that one can absorb using four enphased local permutations, each containing $d - 1$ phases; $4(d-1) = 8$. Note that $d^2 - 1 = 4(d-1)$ has a solution only for $d = 3$ and thus such results about LU equivalence about enphased 2-unitary permutations in $d = 3$ do not hold for $d > 3$.

2. LU equivalence of 2-unitaries in $d = 3$

Dynamical maps are very efficient in yielding 2-unitaries for local Hilbert-space dimension $d = 3$ and $d = 4$ from random-seed unitaries. The 2-unitaries so obtained do not have an evident simple structure, as do 2-unitary permutations. It is natural to ask if these are

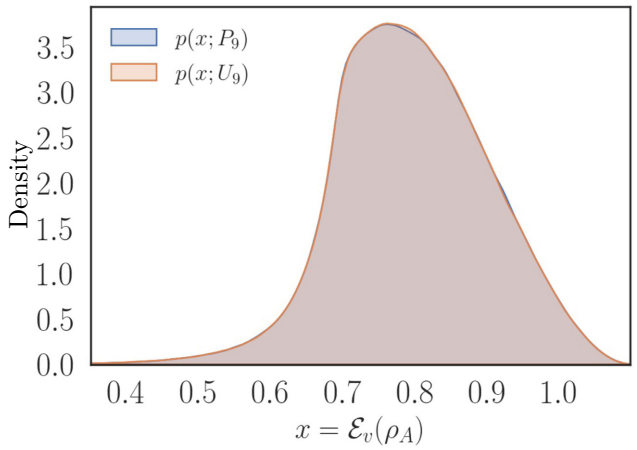

FIG. 7. The two-qutrit case $d^2 = 9$. The distributions $p(x;U)$ of entanglement obtained from the action of 9×9 unitaries U on Haar-distributed product states. Two distributions, one corresponding to the 2-unitary permutation matrix P_9, Eq. (77) and the other a 2-unitary U_9 obtained from the map with a random seed, are shown. These two are numerically indistinguishable and we cannot find a different distribution than the one shown here for the $O(10^3)$ 2-unitaries obtained from the map.

LU equivalent to each other. For the purposes of LU equivalence, we compare the entanglement distributions of 2-unitaries obtained from the map, $p(x;U)$, with that of the 2-unitary permutation matrix, $p(x;P_9)$. We find that the von Neumann entropy is a good measure to highlight the differences in the distributions; in particular, it performs better than the linear entropy and hence we use it. The von Neumann entropy of the single-qudit reduced-density matrix of $|\psi\rangle_{AB}$ [see Eq. (74)] is defined as

$$\mathcal{E}_v(\rho_A) = -\mathrm{tr}(\rho_A \log \rho_A).$$

The distributions $p(x;P_9)$ and $p(x;U_9)$ from a 2-unitary U_9 are shown in Fig. 7. The matrix U_9 is obtained using a random seed in the dynamical map $\mathcal{M}_{\Gamma R}$. Surprisingly, both the distributions are indistinguishable for these 2-unitaries, although their origins and forms are very different. We check entanglement distributions for $O(10^3)$ 2-unitaries obtained from the map but cannot find a different distribution from that of the 2-unitary permutation matrix. In fact, in most cases we can transform the 2-unitaries obtained from the map, using random seeds, into 2-unitary permutation matrices using appropriate local transformations in $\mathcal{U}(3) \otimes \mathcal{U}(3)$. Based on overwhelming numerical evidence, we propose the following conjecture.

Conjecture 1: *All 2-unitaries of order 9 are LU equivalent to P_9.*

C. 2-unitaries in $d = 4$

1. Permutations

The total number of 2-unitary permutations of size 16 is $2 \times 3456 = 6912$. By performing a direct exhaustive search over local permutations, quite remarkably—even in this case—it turns out that *all* 6912 2-unitary permutations are LU equivalent and thus lead to the following proposition.

Proposition 3: *There is only one LU class of 2-unitary permutations of order 16.*

We choose the following 2-unitary permutation matrix as a representative of the LU-equivalent class of 2-unitary permutations of order 16:

$$P_{16} = \left(\begin{array}{cccc|cccc|cccc|cccc}
1 & . & . & . & . & . & . & . & . & . & . & . & . & . & . & . \\
. & . & . & . & . & 1 & . & . & . & . & . & . & . & . & . & . \\
. & . & . & . & . & . & . & . & . & . & 1 & . & . & . & . & . \\
. & . & . & . & . & . & . & . & . & . & . & . & . & . & . & 1 \\
\hline
. & . & . & . & . & . & . & 1 & . & . & . & . & . & . & . & . \\
. & . & 1 & . & . & . & . & . & . & . & . & . & . & . & . & . \\
. & . & . & . & . & . & . & . & . & . & . & . & . & 1 & . & . \\
. & . & . & . & . & . & . & . & 1 & . & . & . & . & . & . & . \\
\hline
. & . & . & . & . & . & . & . & . & 1 & . & . & . & . & . & . \\
. & . & . & . & . & . & . & . & . & . & . & . & 1 & . & . & . \\
. & . & . & 1 & . & . & . & . & . & . & . & . & . & . & . & . \\
. & . & . & . & . & . & 1 & . & . & . & . & . & . & . & . & . \\
\hline
. & . & . & . & . & . & . & . & . & . & . & . & . & . & 1 & . \\
. & . & . & . & . & . & . & . & . & . & . & 1 & . & . & . & . \\
. & . & . & . & 1 & . & . & . & . & . & . & . & . & . & . & . \\
. & 1 & . & . & . & . & . & . & . & . & . & . & . & . & . & .
\end{array}\right). \tag{79}$$

Using $(4!)^4 = 3,31,776$ possible local permutations, each 2-unitary permutation is obtained 48 times and therefore all $331776/48 = 6912$ are taken into account.

2. Entangled OLSs of size 4: A new example of AME(4, 4)

Although there is only one LU class of 2-unitary permutations of order 16, we give an explicit example of a 2-unitary orthogonal matrix that is not LU equivalent to any 2-unitary permutation. This is obtained via the nonlinear map $\mathcal{M}_{\Gamma R}$ given in Eq. (23) with a permutation seed, and is given by

$$O_{16} = \frac{1}{2}\left(\begin{array}{cccc|cccc|cccc|cccc}
1 & . & . & . & . & 1 & . & . & . & . & -1 & . & . & . & . & -1 \\
. & 1 & . & . & -1 & . & . & . & . & . & . & -1 & . & . & -1 & . \\
. & . & -1 & . & . & . & . & 1 & -1 & . & . & . & . & -1 & . & . \\
. & . & . & -1 & . & . & 1 & . & . & 1 & . & . & 1 & . & . & . \\
\hline
. & 1 & . & . & -1 & . & . & . & . & . & . & 1 & . & . & 1 & . \\
-1 & . & . & . & . & 1 & . & . & . & . & 1 & . & . & . & . & -1 \\
. & . & . & -1 & . & . & 1 & . & . & -1 & . & . & -1 & . & . & . \\
. & . & -1 & . & . & . & . & -1 & 1 & . & . & . & . & -1 & . & . \\
\hline
. & . & -1 & . & . & . & . & -1 & -1 & . & . & . & . & 1 & . & . \\
. & . & . & 1 & . & . & 1 & . & . & -1 & . & . & 1 & . & . & . \\
-1 & . & . & . & . & -1 & . & . & . & . & -1 & . & . & . & . & -1 \\
. & -1 & . & . & -1 & . & . & . & . & . & . & -1 & . & . & 1 & . \\
\hline
. & . & . & -1 & . & . & -1 & . & . & -1 & . & . & 1 & . & . & . \\
. & . & 1 & . & . & . & . & -1 & -1 & . & . & . & . & -1 & . & . \\
. & 1 & . & . & 1 & . & . & . & . & . & . & -1 & . & . & 1 & . \\
1 & . & . & . & . & -1 & . & . & . & . & 1 & . & . & . & . & -1
\end{array}\right). \tag{80}$$

This matrix can be written in a compact form as

$$O_{16} = P_{16}^T D_4 P_{16}, \tag{81}$$

where D_4 is a block-diagonal matrix consisting of four 4×4 Hadamard matrices. Each row or column of O_{16} contains four nonzero entries being equal to either $1/2$ or $-1/2$ and is such that its eighth power is equal to the identity $O_{16}^8 = \mathbb{I}$. To show that O_{16} is indeed not LU equivalent to P_{16}, we compare the entanglement distributions $p(x; O_{16})$ and $p(x; P_{16})$. The distributions, shown in Fig. 8, are clearly distinguishable: $p(x; O_{16}) \neq p(x; P_{16})$ and thus $O_{16} \overset{\text{LU}}{\not\sim} P_{16}$. Entanglement distributions for a large number of generic 2-unitaries obtained by applying the dynamical map $\mathcal{M}_{\Gamma R}$ on random-seed unitaries do not result in any distinguishable distributions other than the ones shown in Fig. 8. This suggests that there are at least three LU classes of 2-unitaries in $d^2 = 16$. The representatives of these three LU classes are as follows: (i) P_{16}, given by Eq. (79); (ii) enphased P_{16}—$P'_{16} = D_1\ P_{16}\ D_2$, where D_1 and D_2 are diagonal unitaries with arbitrary phases; and (iii) O_{16}, given by Eq. (80). Note that P_{16} and P'_{16} are not LU equivalent in general and thus the corresponding AME states of minimal support are not LU equivalent.

Each row or column of O_{16} treated as a pure state in $\mathcal{H}_4 \otimes \mathcal{H}_4$ is maximally entangled and thus the underlying combinatorial design corresponding to O_{16} does not factor into the separable structures $\mathcal{K}$ and $\mathcal{L}$ defined in Eq. (66). Also note that each 4×4 block in Eq. (80) is unitary up to a scale factor and thus the rows or columns

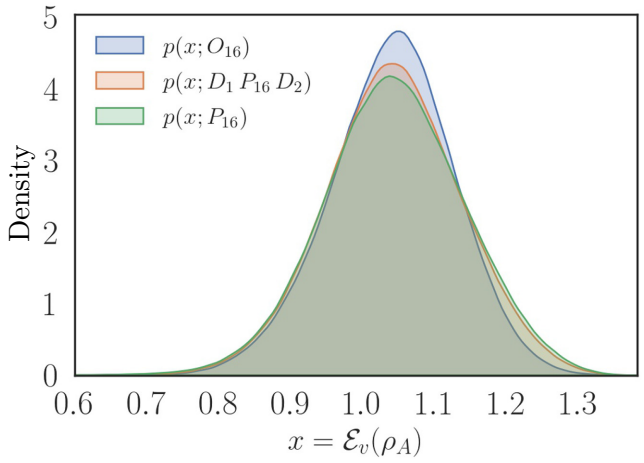

FIG. 8. The two-ququad case $d^2 = 16$. The distributions $p(x; U)$ of entanglement corresponding to the 2-unitary permutation matrix $U = P_{16}$ [Eq. (79)] and the 2-unitary orthogonal matrix $U = O_{16}$ [Eq. (80)]. The distributions are clearly distinguishable and show that P_{16} and O_{16} are not LU equivalent. Also shown is the entanglement distribution corresponding to enphased P_{16}—$D_1 P_{16} D_2$, where D_1 and D_2 are diagonal unitaries—which is not LU equivalent to either P_{16} or O_{16}.

of O_{16}^R are also maximally entangled states in $\mathcal{H}_4 \otimes \mathcal{H}_4$. Similar entangled combinatorial structures corresponding to a 2-unitary of size 36 have been referred to as entangled OQLSs in Ref. [56] in which entangled OQLSs of size 6 have been found in Sec. VI B. Based on our discussion in the previous section on 2-unitaries of size 9 and the known fact that there are no 2-unitaries of size 4, $d = 4$ seems to be the smallest possible dimension in which entangled OLSs exist.

This allows us to construct a new kind of AME state of four ququads; AME(4, 4), which is not LU equivalent to an AME state of minimal support constructed from P_{16}. The corresponding AME state written in the computational basis is given by

$$|O_{16}\rangle = \sum_{i,j,k,l=1}^{4} (O_{16})_{ij,kl} \, |ijkl\rangle \, . \tag{82}$$

The tensor $T_{ijkl} = (O_{16})_{ij,kl}$ is a perfect tensor [49], the nonzero entries of which are given by Eq. (80). To our knowledge, this is the simplest AME state that is not derived from a classical design or is equivalent to one (for equivalence among AME states, see, e.g., Refs. [61,93]). Thus it qualifies as a younger cousin of AME(4,6), which is a genuine OQLS [56]. However, unlike the golden state AME(4,6), this is purely real. Earlier constructions of ququad AME states have a much larger number of particles [93].

We perform several local unitary transformations on O_{16} and reduce the number of its nonzero entries or, equivalently, the support of the AME state given by Eq. (82), from 64 to 42, although the transformed matrix has entries other than $\pm 1/2$. The transformed matrix has two unentangled columns and therefore O_{16} is not a universal entangler.

VII. ENTANGLING PROPERTIES OF DUAL AND T-DUAL PERMUTATION MATRICES

Permutation matrices form an important class of entangling unitary operators [60]. In this section, we study the entangling properties of dual and T-dual permutation matrices on $\mathcal{H}_d \otimes \mathcal{H}_d$, which are special subsets of the permutation group $P(d^2)$. Dual-unitary permutation matrices have recently been explored in Ref. [89] and used as building blocks of quantum circuits with interesting dynamical behavior [50]. Two permutation matrices, P_1 and P_2, have been defined in Ref. [60] to belong to the same *entangling class* if they have the same entangling power, $e_p(P_1) = e_p(P_2)$. Two LU-equivalent permutation matrices always belong to the same entangling class but permutation matrices belonging to the same entangling power need not be LU equivalent. For the sake of convenience, we write the permutation matrix in terms of the column number of the only nonzero entry in each row. For example, in this notation, P_9 given by Eq. (77) is written as $P_9 = \{1, 5, 9, 6, 7, 2, 8, 3, 4\}$, corresponding to the permutation $\pi : \{1, 2, 3, 4, 5, 6, 7, 8, 9\} \to \{\pi(1) = 1, \pi(2) = 5, \ldots, \pi(8) = 3, \pi(9) = 4\}$.

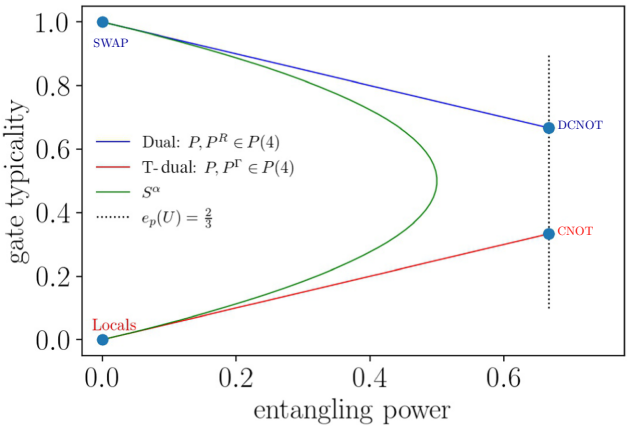

FIG. 9. The two-qubit case $d^2 = 4$. The entangling power versus the gate typicality of all permutations $P(4)$, treated as two-qubit gates. The number of entangling classes, those with different entangling powers, is 2.

A. Dual-unitary and T-dual permutations in $d = 2$ and $d = 3$

We list all possible entangling classes for dual-unitary permutations in $P(d^2)$ for $d = 2$ and $d = 3$.

In the *two-qubit case*, the corresponding permutation group is $P(4)$. The projection of $P(4)$ on e_p-g_t plane is shown in Fig. 9. There are four distinct points corresponding to 24 possible permutations of order 4, treated as two-qubit gates, on the e_p-g_t plane and every permutation matrix is either dual or T dual. The number of entangling classes is only two and these are listed in Table II.

In the *two-qutrit case*, the corresponding permutation group is $P(9)$. The projection of $P(9)$, treated as two-qutrit gates, on the e_p-g_t plane is shown in Fig. 10. There are only 60 distinct points on the e_p-g_t plane from the $9! = 3,62,000$ possible permutation matrices of order 9.

It has been shown in Ref. [94] that there are 18 LU classes of T-dual (or, equivalently, dual-unitary) permutation matrices. A representative permutation from each LU class is also listed therein. These LU classes are listed in Table III along with their entangling powers. Therefore,

TABLE II. The entangling and LU classes of dual (equivalently, T dual) permutations in $P(4)$.

$e_p(P)$	No. of LU classes
0	1
2/3	1

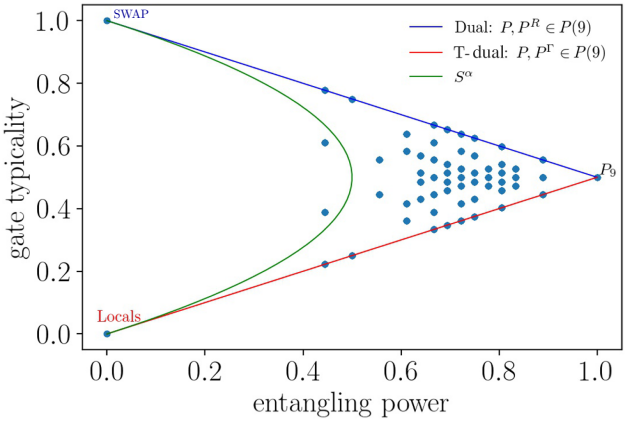

FIG. 10. The two-qutrit case $d^2 = 9$. The entangling power versus the gate typicality of all 9! permutations $P(9)$, treated as two-qutrit gates. The number of entangling classes corresponding to dual (and, equivalently, T dual) permutation matrices is 10.

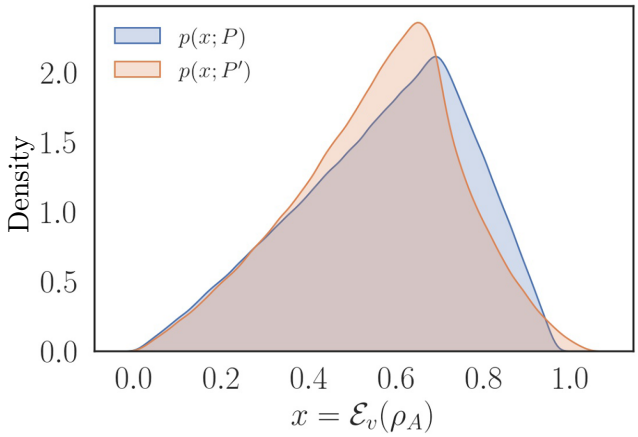

FIG. 11. The entanglement distributions obtained for P and P' permutation matrices of size 9 belonging to two LUS classes (see the text) corresponding to the entangling class with $e_p(U) = 2/3$. The distinguishabiliity of the distributions implies that P and P' are not LU equivalent.

the number of entangling classes corresponding to dual-unitary (and, equivalently, T-dual) permutation matrices is 10.

Except for three entangling classes [corresponding to $e_p(P) = 0$, $e_p(P) = 8/9$, and $e_p(P) = 1$], there is more than one LU class. Taking permutations from two different LU classes with the same entangling power (say, $e_p(P) = 1/2$), we observe that these produce the same entanglement distributions $p(x; U)$. This suggests that these LU-inequivalent permutations with the same entangling power and gate typicality might be connected by the SWAP gate. Indeed, we find that according to the LUS classification defined in Eq. (76) with $a = b = 1$, there are only 11 LUS classes, i.e., two permutations P and P' belonging to the same entangling class but different LU classes are related (up to local permutations) as $P' = SPS$, where S is the SWAP gate. This is the case for all entangling classes in Table III with more than one LU classes except for the entangling class $e_p(U) = 2/3$.

TABLE III. The entangling, LU, and LUS classes of dual (equivalently, T-dual) permutations in $P(9)$.

S.No.	$e_p(P)$	No. LU classes	No. LUS classes
1	0	1	1
2	4/9	2	1
3	1/2	2	1
4	2/3	3	**2**
5	25/36	2	1
6	13/18	2	1
7	3/4	2	1
8	29/36	2	1
9	8/9	1	1
10	1	1	1
Total		18	11

The entangling class $e_p(U) = 2/3$ is special and has two LUS classes. Representative permutations written in compact form as $P = \{1, 4, 8, 2, 5, 7, 6, 3, 9\}$ and $P' = \{1, 4, 9, 2, 5, 8, 6, 3, 7\}$ from both LUS classes produce the distinguishable entanglement distributions shown in Fig. 11. The LU inequivalence between P and P' can also be seen via the singular values of P^Γ and P'^Γ, which are LUIs [see Eq. (17)]; the singular values of P^Γ and P'^Γ are $\{2, 2, 1\}$ and $\left\{\sqrt{5}, \sqrt{2}, \sqrt{2}\right\}$, respectively. This leads us to the strong suspicion that the equality of entanglement distributions may be a sufficient condition for LUS equivalence, i.e., $p(x; U) = p(x; U')$ if and only if $U \overset{\text{LUS}}{\sim} U'$.

An interesting fact that we observe is that with von Neumann entropy as a measure of entanglement, the averages of the distributions obtained for these permutations differ slightly; for P, $\overline{\mathcal{E}_v(\rho_A)} \approx 0.57$, while for P', $\overline{\mathcal{E}_v(\rho_A)} \approx 0.55$, taking into account 10^6 realizations of product states in both cases. Note that if the linear entropy is taken as a measure, then the averages must be equal according to the definition of the entangling power [37]. This suggests the role of other unknown LU invariants besides $E(U)$ and $E(US)$, which determine the average of the entanglement distribution when von Neumann entropy is taken as a measure of entanglement.

It is to be noted that out of 18 possible LU classes *only one* corresponds to the entangling class $e_p(P) = 1$ of 2-unitary permutations. As a consequence of this, all 72 possible 2-unitary permutations of order 9 are locally equivalent, which is consistent with Proposition 2.

B. Numerical results for $d > 3$

The total possible number of LU classes of dual or, T-dual, permutations in $P(d^2)$ for $d > 3$ is not known. The number of entangling classes is also not known, as an exhaustive enumeration of such permutations is prohibitively large. To obtain a lower bound on the possible number of entangling classes corresponding to dual-unitary permutations of size 16, we numerically search over permutations in the vicinity of different permutations such as SWAP and 2-unitary gates. The results obtained from such a search over around 1.2×10^7 permutations of size 16 (out of a possible $16! \sim 10^{13}$) are shown in Fig. 12. We obtain 56 entangling classes corresponding to dual or, equivalently, T-dual permutations. This provides a weak lower bound on the number of LU-inequivalent classes for dual-unitary permutations of size 16. Note that one of the entangling classes is $e_p(U) = 1$, corresponding to 2-unitary permutations for which there is only one LU-equivalence class (see Proposition 3).

We end this section by showing that there exists more than one LU class for 2-unitary permutations in $d > 4$. An easy way to see this is by comparing entanglement distributions of 2-unitary permutation $P \in P(d^2)$ and their realignment $P^R \in P(d^2)$. This is shown in Fig. 13 for a 2-unitary permutation in $d = 5$ given by

$$P_{25} = \{1, 7, 13, 19, 25, 22, 3, 9, 15, 16, 18, 24, 5, 6, 12, 14, 20, 21, 2, 8, 10, 11, 17, 23, 4\},$$
$$P_{25}^R = \{1, 7, 13, 19, 25, 8, 14, 20, 21, 2, 15, 16, 22, 3, 9, 17, 23, 4, 10, 11, 24, 5, 6, 12, 18\}. \quad (83)$$

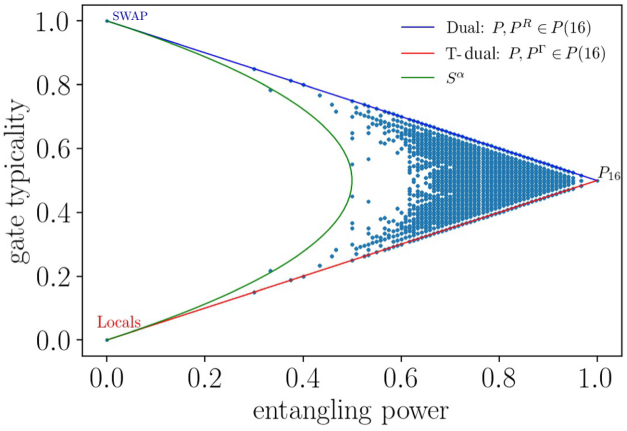

FIG. 12. The two-ququad case $d^2 = 16$. The entangling power versus the gate typicality of 1.2×10^7 permutations (out of a total of $16! \approx 10^{13}$ permutations), treated as two-ququad gates. the number of entangling classes corresponding to dual (and, equivalently, T-dual) permutation matrices obtained from our numerical search is found to be 56.

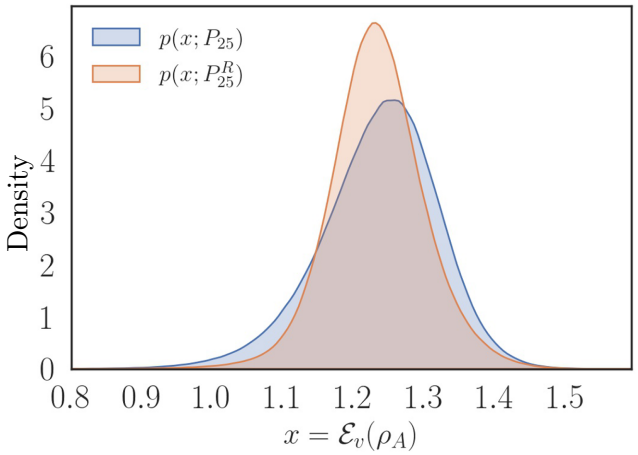

FIG. 13. Case of $d^2 = 25$. The entanglement distributions of 2-unitary permutation P_{25} [see Eq. (83)] and its realignment P_{25}^R, which is also a 2-unitary. The distributions are clearly distinguishable: $p(x; P_{25}) \neq p(x; P_{25}^R)$ and this shows that $P_{25} \overset{\text{LU}}{\not\approx} P_{25}^R$.

The entanglement distributions are different; $p(x; P_{25}) \neq p(x; P_{25}^R)$ and this establishes that they are not LU equivalent. Recall that one cannot justify LU inequivalence between 2-unitaries based on the singular values of their reshuffled and partially transposed rearrangements as they are all maximized, being equal to 1. We check the entanglement distributions for 100 2-unitary permutations of size 25 together with their different rearrangements but find only two different distributions, shown in Fig. 13. Thus the total number of LU and LUS classes for 2-unitary permutations in $d = 5$ remains unknown but it is certainly greater than 1. Similarly, in $d = 7$, $d = 8$, and $d = 9$, we observe only two different distributions corresponding to 2-unitary permutations and their rearrangements.

A consequence of having more than one LU class of enphased 2-unitary permutations in $d > 3$ is that it results in minimal-support AME states that are not LU equivalent. Our results thus contradict Conjecture 2 in Ref. [61], which, particularly for four-party states, implies that there is only one LU class of AME states of minimal support. As we illustrate in Figs. 8 and 13, there exists more than one LU class of AME states of minimal support for $d = 4$ and $d = 5$.

Assuming that 2-unitary permutations belonging to the same LU class are related by local permutations, it can be seen that there are more than one LU class of 2-unitary permutations for $d = 7$, $d = 8$, and $d = 9$. It follows from the fact that the number of possible OLS known for these cases (see A072377, Ref. [92]) exceeds the number of OLS that can be obtained from a 2-unitary permutation P using local permutations; $(p_1 \otimes p_2)P(p_3 \otimes p_4)$. It is to be noted that all $(d!)^4$ number of OLS so obtained are not all different. Interestingly, in $d = 5$, we find that although

$(5!)^4 = 207360000$ exceeds the number of possible OLS (equal to 3110400), the latter is not a factor of the former, unlike the cases $d = 3$ and $d = 4$.

VIII. SUMMARY AND DISCUSSION

Despite several constructions of the set of dual-unitary operators, the complete characterization for an arbitrary local Hilbert-space dimension remains an open problem. In Ref. [47], we have proposed a nonlinear iterative map that produces dual-unitary operators from arbitrary-seed unitaries. The map acts as a dynamical system in the space of bipartite unitary operators. In this work, we study the period-2 fixed points of the map, which are dual-unitary operators, and provide a stochastic generalization of the map, which produces structured fixed points that are dual unitaries. Complete characterization of the fixed points of all orders remains to be understood and makes the map a novel dynamical system in its own right. For two-qubit gates, using the canonical or Cartan decomposition, we analytically study the convergence rates for various initial conditions. However, convergence of the map in local Hilbert-space dimension $d > 2$ remains an unsolved problem.

The subset of dual-unitary operators having maximum entangling power is that of 2-unitary operators. The 2-unitary permutation operators can be constructed from combinatorial designs called OLSs. The nonexistence of OLSs of size 6 motivates us to look for general quantum combinatorial designs corresponding to 2-unitary operators, as have recently been found in Ref. [56] for local dimension $d = 6$. The problem of finding such quantum combinatorial designs reduces to finding the 2-unitary operators that are not LU equivalent to any 2-unitary permutation matrix. From our extensive numerical searches using the dynamical map and known constructions of 2-unitaries, we cannot find any such quantum design for local dimension $d = 3$. All 2-unitary permutation operators of size 9 are LU equivalent to each other. Based on these results, we conjecture that *all* 2-unitary operators of size 9, not just permutations, are LU equivalent to each other. If true, this implies that there is just *one* 2-unitary two-qutrit gate up to LU equivalence.

Methods to ascertain LU equivalence between bipartite unitary operators are not known in general. For unitary operators with identical values of known LUIs such as the entangling power and the gate typicality, the problem of LU equivalence becomes harder. In this paper, we propose a necessary criterion for distinguishing LU-inequivalent 2-unitary operators based on the entanglement distribution that these produce. Using the iterative map, we find a 2-unitary operator for local dimension $d = 4$ that is LU inequivalent to any 2-unitary permutation of the same size. Thus, this qualifies as a genuine 2-unitary quantum design in the lowest possible dimension, as they do not exist for $d = 2$ and, as far as we know, for $d = 3$. This also implies that we display an explicit example of an AME(4, 4) state that is not LU equivalent to AME(4, 4), of minimal support. We show that for $d = 5$, there are at least two LU classes of 2-unitary permutations and thus there are two LU-inequivalent AME states of minimal support. The consequences of these new examples of AME states for quantum error correction are an interesting direction and are left for future studies. The stochastic local operations and classical communication (SLOCC) equivalence of LU-inequivalent four-party AME states found in this work for $d > 3$ is an interesting problem and is left for future studies.

Note added.—Recently, we became aware of Ref. [95], in which a criterion for determining the local unitary equivalence of operators is presented that involves an exponential (in local dimension) set of invariants.

ACKNOWLEDGMENTS

We are grateful to Balázs Pozsgay for discussions on dual unitarity and its connections to biunitarity. We thank Karol Życzkowski and Adam Burchardt for comments on a preliminary version and for illuminating remarks on the issue of LU equivalence. We are thankful to Vijay Kodiyalam for pointing out Ref. [95] and discussions around it. Rohan Narayan's and Shrigyan Brahmachari's inputs and questions were much appreciated. This work was partially funded by the Center for Quantum Information Theory in Matter and Spacetime, IIT Madras, and the Department of Science and Technology, Government of India, under Grant No. DST/ICPS/QuST/Theme-3/2019/Q69. S.A. acknowledges the Institute postdoctoral fellowship program of IIT Madras for funding during the initial stages of this work.

APPENDIX A: DETAILS ABOUT THE MAP IN THE TWO-QUBIT CASE

In the two-qubit case, the Cartan form of any unitary [see Eq. (27)] can be written as

$$U_0 = \begin{pmatrix} e^{-ic_3^{(0)}} c_-^{(0)} & 0 & 0 & -ie^{-ic_3^{(0)}} s_-^{(0)} \\ 0 & e^{ic_3^{(0)}} c_+^{(0)} & -ie^{ic_3^{(0)}} s_+^{(0)} & 0 \\ 0 & -ie^{ic_3^{(0)}} s_+^{(0)} & e^{ic_3^{(0)}} c_+^{(0)} & 0 \\ -ie^{-ic_3^{(0)}} s_-^{(0)} & 0 & 0 & e^{-ic_3^{(0)}} c_-^{(0)} \end{pmatrix}, \tag{A1}$$

where

$$c_\pm^{(0)} = \cos(c_1^{(0)} \pm c_2^{(0)}); \qquad s_\pm^{(0)} = \sin(c_1^{(0)} \pm c_2^{(0)}).$$

The unitary operator U in its canonical decomposition has four parameters. Let $\alpha_0 = e^{-ic_3^{(0)}} c_-^{(0)}, \beta_0 = -ie^{-ic_3^{(0)}} s_-^{(0)}$,

$\gamma_0 = -ie^{ic_3^{(0)}} s_+^{(0)}$, and $\delta_0 = e^{ic_3^{(0)}} c_+^{(0)}$. Then, the Eq. (A1) can be written as

$$U_0 = \begin{pmatrix} \alpha_0 & 0 & 0 & \beta_0 \\ 0 & \delta_0 & \gamma_0 & 0 \\ 0 & \gamma_0 & \delta_0 & 0 \\ \beta_0 & 0 & 0 & \alpha_0 \end{pmatrix}. \tag{A2}$$

The $\mathcal{M}_R$ map can now be studied analytically by applying it to the two-qubit unitary operators in its Cartan form [see Eq. (A2)]. The action of linear map R on U_0 defined in Eq. (A2) results in

$$U_0^R = \begin{pmatrix} \alpha_0 & 0 & 0 & \delta_0 \\ 0 & \beta_0 & \gamma_0 & 0 \\ 0 & \gamma_0 & \beta_0 & 0 \\ \delta_0 & 0 & 0 & \alpha_0 \end{pmatrix}. \tag{A3}$$

The polar decomposition of the matrix U_0^R, which is given by $U_0^R = U_1 H$, where U_1 is unitary and $H = \sqrt{U^{R\dagger} U^R}$, is given by

$$H = \frac{1}{2} \begin{pmatrix} |\alpha_0 - \delta_0| + |\alpha_0 + \delta_0| & 0 & 0 & -|\alpha_0 - \delta_0| + |\alpha_0 + \delta_0| \\ 0 & |\beta_0 - \gamma_0| + |\beta_0 + \gamma_0| & -|\beta_0 - \gamma_0| + |\beta_0 + \gamma_0| & 0 \\ 0 & -|\beta_0 - \gamma_0| + |\beta_0 + \gamma_0| & |\beta_0 - \gamma_0| + |\beta_0 + \gamma_0| & 0 \\ -|\alpha_0 - \delta_0| + |\alpha_0 + \delta_0| & 0 & 0 & |\alpha_0 - \delta_0| + |\alpha_0 + \delta_0| \end{pmatrix}. \tag{A4}$$

The unitary $U_1 = U_0^R H^{-1}$ is given by

$$U_1 = \begin{pmatrix} \alpha_0\alpha_+ + \delta_0\alpha_- & 0 & 0 & \alpha_0\alpha_- + \delta_0\alpha_+ \\ 0 & \beta_0\beta_+ + \gamma_0\beta_- & \beta_0\beta_- + \gamma_0\beta_+ & 0 \\ 0 & \gamma_0\beta_+ + \beta_0\beta_- & \gamma_0\beta_- + \beta_0\beta_+ & 0 \\ \alpha_0\alpha_- + \delta_0\alpha_+ & 0 & 0 & \alpha_0\alpha_+ + \delta_0\alpha_- \end{pmatrix}, \tag{A5}$$

where $\alpha_\pm$ and $\beta_\pm$ are given as

$$\alpha_\pm = \frac{|\alpha_0 - \delta_0| \pm |\alpha_0 + \delta_0|}{2|\alpha_0 - \delta_0||\alpha_0 + \delta_0|}, \qquad \beta_\pm = \frac{|\beta_0 - \gamma_0| \pm |\beta_0 + \gamma_0|}{2|\beta_0 - \gamma_0||\beta_0 + \gamma_0|}. \tag{A6}$$

Note that although $U_0 \in \mathcal{SU}(4)$, U_1 given by Eq. (A5) need not be in $\mathcal{SU}(4)$ in general. The mapping between $\alpha_0, \beta_0, \gamma_0, \delta_0$ of U_0 and $\alpha_1', \beta_1', \gamma_1', \delta_1'$ of U_1 is

$$\begin{aligned} \alpha_1' &= \frac{(\alpha_0 + \delta_0)|\alpha_0 - \delta_0| + (\alpha_0 - \delta_0)|\alpha_0 + \delta_0|}{2|\alpha_0 - \delta_0||\alpha_0 + \delta_0|}, \\ \beta_1' &= \frac{(\alpha_0 + \delta_0)|\alpha_0 - \delta_0| - (\alpha_0 - \delta_0)|\alpha_0 + \delta_0|}{2|\alpha_0 - \delta_0||\alpha_0 + \delta_0|}, \\ \gamma_1' &= \frac{(\beta_0 + \gamma_0)|\beta_0 - \gamma_0| - (\beta_0 - \gamma_0)|\beta_0 + \gamma_0|}{2|\beta_0 - \gamma_0||\beta_0 + \gamma_0|}, \\ \delta_1' &= \frac{(\beta_0 + \gamma_0)|\beta_0 - \gamma_0| + (\beta_0 - \gamma_0)|\beta_0 + \gamma_0|}{2|\beta_0 - \gamma_0||\beta_0 + \gamma_0|}. \end{aligned} \tag{A7}$$

The above set of equations, written in a compact form as

$$\begin{pmatrix} \alpha_1' \\ \beta_1' \\ \gamma_1' \\ \delta_1' \end{pmatrix} = \begin{pmatrix} \alpha_+ & 0 & 0 & \alpha_- \\ \alpha_- & 0 & 0 & \alpha_+ \\ 0 & \beta_- & \beta_+ & 0 \\ 0 & \beta_+ & \beta_- & 0 \end{pmatrix} \begin{pmatrix} \alpha_0 \\ \beta_0 \\ \gamma_0 \\ \delta_0 \end{pmatrix}, \tag{A8}$$

depicts the nonlinear nature of the map.

APPENDIX B: PROOFS OF THE FIXED-POINT THEOREMS IN THE TWO-QUBIT CASE

1. Proof of Theorem 1

Proof. Let U_0 be a two-qubit gate of the form given in Eq. (32). If U_0 is a fixed point of the $\mathcal{M}_R$ map,

$$\mathcal{M}_R[U_0] = U_1 = U_0. \tag{B1}$$

As this implies that U_1 is also in $\mathcal{SU}(4)$, $\chi_1 = 0$. Using Eq. (34), the fixed-point condition $\mathcal{M}_R[U_0] = U_0$ can be written as

$$\alpha_0 = \frac{1}{2}[(k_+^{(0)} + k_-^{(0)})\alpha_0 + (k_+^{(0)} - k_-^{(0)})\delta_0], \tag{B2a}$$

$$\beta_0 = \frac{1}{2}[(k_+^{(0)} - k_-^{(0)})\alpha_0 + (k_+^{(0)} + k_-^{(0)})\delta_0], \tag{B2b}$$

$$\gamma_0 = \frac{1}{2}[(l_+^{(0)} - l_-^{(0)})\beta_0 + (l_+^{(0)} + l_-^{(0)})\gamma_0], \tag{B2c}$$

$$\delta_0 = \frac{1}{2}[(l_+^{(0)} + l_-^{(0)})\beta_0 + (l_+^{(0)} - l_-^{(0)})\gamma_0], \tag{B2d}$$

where $k_\pm^{(0)} = 1/|\alpha_0 \pm \delta_0|$ and $l_\pm^{(0)} = 1/|\beta_0 \pm \gamma_0|$. From the unitarity of U_0, it follows that $\mathrm{Re}(\alpha_0\beta_0^*) = \mathrm{Re}(\gamma_0\delta_0^*) = 0$. Multiplying Eq. (B2a) by γ_0^*, Eq. (B2c) by α_0^* in Eq. (B2), and taking real parts, we obtain $k_+^{(0)} + k_+^{(0)} = l_+^{(0)} + l_+^{(0)} = 2$. Similarly, multiplying Eq. (B2a) by β_0^* and taking the real parts, we obtain

$$(k_+^{(0)} - k_-^{(0)})\mathrm{Re}[\delta_0\beta_0^*] = 0. \tag{B3}$$

Therefore, either $k_+^{(0)} = k_-^{(0)}$ or $\mathrm{Re}[\delta_0\beta_0^*] = 0$. For $k_+^{(0)} = k_-^{(0)}$, together with the condition $k_+^{(0)} + k_+^{(0)} = 2$, from Eq. (B2b), it follows that $\beta_0 = \delta_0$. For U_0 with $\beta_0 = \delta_0 \neq 0$, it is can be shown that $\gamma_0 = \pm\alpha_0$ using the unitarity of U_0. Therefore, U_0 is of the form

$$U_0 = \begin{pmatrix} \alpha_0 & 0 & 0 & \beta_0 \\ 0 & \beta_0 & \pm\alpha_0 & 0 \\ 0 & \pm\alpha_0 & \beta_0 & 0 \\ \beta_0 & 0 & 0 & \alpha_0 \end{pmatrix}, \tag{B4}$$

which satisfies $U_0^R = U_0$ and thus is a self-dual unitary. From Eqs. (B2b) and (B2d), using the unitarity of U_0 together with $k_+^{(0)} + k_+^{(0)} = l_+^{(0)} + l_+^{(0)} = 2$, it follows that $|\beta_0|^2 = |\delta_0|^2 = \mathrm{Re}(\beta_0\delta_0^*)$. Therefore, the other condition $\mathrm{Re}(\beta_0\delta_0^*) = 0$ in Eq. (B3) is satisfied only when $\beta_0 = \delta_0 = 0$. In this case, U_0 is of the form

$$U_0 = \begin{pmatrix} \alpha_0 & 0 & 0 & 0 \\ 0 & 0 & \gamma_0 & 0 \\ 0 & \gamma_0 & 0 & 0 \\ 0 & 0 & 0 & \alpha_0 \end{pmatrix}, \tag{B5}$$

where $|\alpha_0| = |\gamma_0| = 1$ and is also self-dual unitary. Hence, all period-1 fixed points of the $\mathcal{M}_R$ map in the two-qubit case are self-dual. ■

The canonical form of the dual unitaries obtained by setting $c_1 = c_2 = \pi/4$ in Eq. (A1) is of the form given in Eq. (B5). Self-dual unitaries of the form given in Eq. (B4) are LU equivalent to the canonical form. For example, $(H \otimes H)U_0(H \otimes H)$, where H is the Hadamard gate—$H = 1/\sqrt{2}\begin{pmatrix} 1 & 1 \\ 1 & -1 \end{pmatrix}$—is of the canonical form, where U_0 is of the form

$$U_0 = \begin{pmatrix} \alpha_0 & 0 & 0 & \beta_0 \\ 0 & \beta_0 & \alpha_0 & 0 \\ 0 & \alpha_0 & \beta_0 & 0 \\ \beta_0 & 0 & 0 & \alpha_0 \end{pmatrix}.$$

2. Proof of Theorem 2

Proof. One way is easy: if U_0 is dual unitary, then $\mathcal{M}_R[U_0] = U_0^R$, as U_0^R is unitary, and therefore $\mathcal{M}_R^2[U_0] = \mathcal{M}_R[U_0^R] = U_0$, i.e., U_0 is a fixed point of the $\mathcal{M}_R^2$ map.

The other direction is as follows. That all fixed points of $\mathcal{M}_R^2$ are dual unitary is nontrivial. Analogous to the period-1 case, the fixed-point equation $\mathcal{M}_R^2[U_0] = U_0$ can be written in terms of matrix elements. The action of $\mathcal{M}_R$ on U_0 leads to U_1, given by

$$U_1 = \begin{pmatrix} \alpha_1 & 0 & 0 & \beta_1 \\ 0 & \delta_1 & \gamma_1 & 0 \\ 0 & \gamma_1 & \delta_1 & 0 \\ \beta_1 & 0 & 0 & \alpha_1 \end{pmatrix},$$

where

$$\alpha_1 = \frac{1}{2}[(k_+^{(0)} + k_-^{(0)})\alpha_0 + (k_+^{(0)} - k_-^{(0)})\delta_0], \tag{B6a}$$

$$\beta_1 = \frac{1}{2}[(k_+^{(0)} - k_-^{(0)})\alpha_0 + (k_+^{(0)} + k_-^{(0)})\delta_0], \tag{B6b}$$

$$\gamma_1 = \frac{1}{2}[(l_+^{(0)} - l_-^{(0)})\beta_0 + (l_+^{(0)} + l_-^{(0)})\gamma_0], \tag{B6c}$$

$$\delta_1 = \frac{1}{2}[(l_+^{(0)} + l_-^{(0)})\beta_0 + (l_+^{(0)} - l_-^{(0)})\gamma_0], \tag{B6d}$$

in which $k_\pm^{(0)} = 1/|\alpha_0 \pm \delta_0|$ and $l_\pm^{(0)} = 1/|\beta_0 \pm \gamma_0|$ and we ignore the overall phase as it does not affect the proof. As $\mathcal{M}_R^2[U_0] := \mathcal{M}_R[\mathcal{M}_R[U_0]] = \mathcal{M}_R[U_1] = U_0$, therefore mapping among the matrix elements is given by

$$\alpha_0 = \frac{1}{2}[(k_+^{(1)} + k_-^{(1)})\alpha_1 + (k_+^{(1)} - k_-^{(1)})\delta_1], \tag{B7a}$$

$$\beta_0 = \frac{1}{2}[(k_+^{(1)} - k_-^{(1)})\alpha_1 + (k_+^{(1)} + k_-^{(1)})\delta_1], \tag{B7b}$$

$$\gamma_0 = \frac{1}{2}[(l_+^{(1)} - l_-^{(1)})\beta_1 + (l_+^{(1)} + l_-^{(1)})\gamma_1], \tag{B7c}$$

$$\delta_0 = \frac{1}{2}[(l_+^{(1)} + l_-^{(1)})\beta_1 + (l_+^{(1)} - l_-^{(1)})\gamma_1], \tag{B7d}$$

where $k_\pm^{(1)} = 1/|\alpha_1 \pm \delta_1|$ and $l_\pm^{(1)} = 1/|\beta_1 \pm \gamma_1|$. Using unitarity constraints $\mathrm{Re}(\alpha_n\beta_n^*) = \mathrm{Re}(\gamma_n\delta_n^*) = 0\,(n = 0, 1)$, we simplify the above set of equations.

Multiplying Eq. (B7a) by γ_1^* and taking real parts, we obtain

$$\mathrm{Re}[\alpha_0\gamma_1^*] = \frac{1}{2}(k_+^{(1)} + k_-^{(1)})\mathrm{Re}[\alpha_1\gamma_1^*]. \tag{B8}$$

Now, multiplying α_0 by the complex conjugate of Eq. (B6c) and taking real parts, we obtain

$$\mathrm{Re}[\alpha_0\gamma_1^*] = \frac{1}{2}(l_+^{(0)} + l_-^{(0)})\mathrm{Re}[\alpha_0\gamma_0^*]. \tag{B9}$$

From Eqs. (B8) and (B9), it follows that

$$\frac{\mathrm{Re}[\alpha_1\gamma_1^*]}{\mathrm{Re}[\alpha_0\gamma_0^*]} = \frac{l_+^{(0)} + l_-^{(0)}}{k_+^{(1)} + k_-^{(1)}}. \tag{B10}$$

Similarly, mutiplying Eq. (B6a) by γ_0^*, the complex conjugate of Eq. (B6c) by α_0, and taking real parts leads to

$$\frac{\mathrm{Re}[\alpha_1\gamma_1^*]}{\mathrm{Re}[\alpha_0\gamma_0^*]} = \frac{k_+^{(0)} + k_-^{(0)}}{l_+^{(1)} + l_-^{(1)}}. \tag{B11}$$

From Eqs. (B10) and (B11), it follows that

$$\frac{l_+^{(0)} + l_-^{(0)}}{k_+^{(1)} + k_-^{(1)}} = \frac{k_+^{(0)} + k_-^{(0)}}{l_+^{(1)} + l_-^{(1)}}. \tag{B12}$$

Multiplying the complex conjugate of Eq. (B7b) by β_1 and taking real parts,

$$\mathrm{Re}[\beta_1\beta_0^*] = \frac{1}{2}(k_+^{(1)} + k_-^{(1)})\mathrm{Re}[\delta_1^*\beta_1]. \tag{B13}$$

Now, multiplying Eq. (B6b) by β_0^* and taking real parts,

$$\mathrm{Re}[\beta_1\beta_0^*] = \frac{1}{2}(k_+^{(0)} + k_-^{(0)})\mathrm{Re}[\delta_0\beta_0^*]. \tag{B14}$$

From Eqs. (B13) and (B14), it follows that

$$\frac{\mathrm{Re}[\delta_1\beta_1^*]}{\mathrm{Re}[\delta_0\beta_0^*]} = \frac{k_+^{(0)} + k_-^{(0)}}{k_+^{(1)} + k_-^{(1)}}. \tag{B15}$$

Similarly, mutiplying Eq. (B6d) by δ_0^*, the complex conjugate of Eq. (B7d) by δ_1, and taking real parts, we obtain

$$\frac{\mathrm{Re}[\delta_1\beta_1^*]}{\mathrm{Re}[\delta_0\beta_0^*]} = \frac{l_+^{(0)} + l_-^{(0)}}{l_+^{(1)} + l_-^{(1)}}. \tag{B16}$$

From Eqs. (B15) and (B16), it follows that

$$\frac{k_+^{(0)} + k_-^{(0)}}{k_+^{(1)} + k_-^{(1)}} = \frac{l_+^{(0)} + l_-^{(0)}}{l_+^{(1)} + l_-^{(1)}}. \tag{B17}$$

From Eqs. (B12) and (B17), it is easy to check that

$$k_+^{(0)} + k_-^{(0)} = l_+^{(0)} + l_-^{(0)}, k_+^{(1)} + k_-^{(1)} = l_+^{(1)} + l_-^{(1)} \tag{B18}$$

Multiplying Eq. (B7a) by γ_0^* and taking real parts, we obtain

$$\begin{aligned}\mathrm{Re}[\alpha_0\gamma_0^*] &= \frac{1}{2}\Big[(k_+^{(1)} + k_-^{(1)})\mathrm{Re}[\alpha_1\gamma_0^*] \\ &\quad + (k_+^{(1)} - k_-^{(1)})\mathrm{Re}[\delta_1\gamma_0^*]\Big], \\ &= \frac{(k_+^{(1)} + k_-^{(1)})(k_+^{(0)} + k_-^{(0)})}{4}\mathrm{Re}[\alpha_0\gamma_0^*] \\ &\quad + \frac{(k_+^{(1)} - k_-^{(1)})(l_+^{(1)} - l_-^{(1)})}{4}\mathrm{Re}[\delta_1\beta_1^*],\end{aligned} \tag{B19}$$

where the second equation is obtained using $\mathrm{Re}[\alpha_1\gamma_0^*] = (k_+^{(0)} + k_-^{(0)})/2\ \mathrm{Re}[\alpha_0\gamma_0^*]$ and $\mathrm{Re}[\delta_1\gamma_0^*] = (l_+^{(1)} - l_-^{(1)})/2\ \mathrm{Re}[\delta_1\beta_1^*]$. Using Eq. (B15) in the above equation, we obtain

$$\begin{aligned}\mathrm{Re}[\alpha_0\gamma_0^*] &= \frac{(k_+^{(1)} + k_-^{(1)})(k_+^{(0)} + k_-^{(0)})}{4}\mathrm{Re}[\alpha_0\gamma_0^*] \\ &\quad + \frac{(k_+^{(1)} - k_-^{(1)})(l_+^{(1)} - l_-^{(1)})}{4}\frac{(k_+^{(0)} + k_-^{(0)})}{(k_+^{(1)} + k_-^{(1)})} \\ &\quad \times \mathrm{Re}[\delta_0\beta_0^*],\end{aligned} \tag{B20}$$

Now, multiplying the complex conjugate of Eq. (B7b) by δ_0 and taking real parts,

$$\begin{aligned}\mathrm{Re}[\beta_0^*\delta_0] &= \frac{1}{2}\Big[(k_+^{(1)} - k_-^{(1)})\mathrm{Re}[\alpha_1^*\delta_0] \\ &\quad + (k_+^{(1)} + k_-^{(1)})\mathrm{Re}[\delta_1^*\delta_0]\Big], \\ &= \frac{(k_+^{(1)} - k_-^{(1)})(l_+^{(1)} - l_-^{(1)})}{4}\mathrm{Re}[\alpha_1^*\gamma_1] \\ &\quad + \frac{(k_+^{(1)} + k_-^{(1)})(l_+^{(1)} + l_-^{(1)})}{4}\mathrm{Re}[\delta_1^*\beta_1],\end{aligned} \tag{B21}$$

where the second equation is obtained using $\mathrm{Re}[\alpha_1^*\delta_0] = (l_+^{(1)} - l_-^{(1)})/2\ \mathrm{Re}[\alpha_1^*\gamma_1]$ and $\mathrm{Re}[\delta_1^*\delta_0] = (l_+^{(1)} + l_-^{(1)})/2\,\mathrm{Re}[\delta_1^*\beta_1]$. Using Eqs. (B10) and (B15) in the above equation, we obtain

$$\begin{aligned}\mathrm{Re}[\beta_0^*\delta_0] &= \frac{(k_+^{(1)} - k_-^{(1)})(l_+^{(1)} - l_-^{(1)})}{4}\frac{(k_+^{(0)} + k_-^{(0)})}{(k_+^{(1)} + k_-^{(1)})}\mathrm{Re}[\alpha_0\gamma_0^*] \\ &\quad + \frac{(k_+^{(0)} + k_-^{(0)})(l_+^{(1)} + l_-^{(1)})}{4}\mathrm{Re}[\delta_0^*\beta_0],\end{aligned} \tag{B22}$$

From Eqs. (B20), (B22) and (B18), we obtain

$$\begin{aligned}&k_+^{(1)} = k_-^{(1)}, l_+^{(1)} = l_-^{(1)}, \\ &(k_+^{(0)} + k_-^{(0)})(k_+^{(1)} + k_-^{(1)}) = (l_+^{(0)} + l_-^{(0)})(l_+^{(1)} + l_-^{(1)}) = 4.\end{aligned} \tag{B23}$$

A similar calculation of $\mathrm{Re}[\alpha_1\gamma_1^*]$ and $\mathrm{Re}[\beta_1\delta_1^*]$ implies that

$$k_+^{(0)} = k_-^{(0)}, l_+^{(0)} = l_-^{(0)},$$
$$(k_+^{(0)} + k_-^{(0)})(k_+^{(1)} + k_-^{(1)}) = (l_+^{(0)} + l_-^{(0)})(l_+^{(1)} + l_-^{(1)}) = 4. \tag{B24}$$

Using Eq. (B24) in Eqs. (B6) and (B7), it follows that $k_\pm^{(n)} = l_\pm^{(n)} = 1$, where $n = 0, 1$, as in the period-1 case. For $k_+^{(1)} = k_-^{(1)} = 1$, $\alpha_1 = \alpha_0, \beta_1 = \delta_0, \gamma_1 = \gamma_0$, and $\delta_1 = \beta_0$. Therefore, $\mathrm{Re}(\alpha_0\delta_0^*) = \mathrm{Re}(\beta_0\gamma_0^*) = 0$, which implies that U_0^R given by

$$U_0^R = \begin{pmatrix} \alpha_0 & 0 & 0 & \delta_0 \\ 0 & \beta_0 & \gamma_0 & 0 \\ 0 & \gamma_0 & \beta_0 & 0 \\ \delta_0 & 0 & 0 & \alpha_0 \end{pmatrix}$$

is also unitary (note that α_0 and γ_0 do not change positions under the realignment operation) and thus U_0 is dual unitary. Hence, $\mathcal{M}_R^2[U_0] = U_0$ implies that U_0 is dual unitary. ■

We assume that α_0, β_0, δ_0, and γ_0 are all nonzero. It is easy to verify from Eqs. (B6)–(B7) that if $\alpha_0 = 0$, then $\gamma_0 = 0$ and if $\beta_0 = 0$, then $\delta_0 = 0$. In the former case, seed unitary is dual unitary of the form

$$U_0^R = \begin{pmatrix} 0 & 0 & 0 & \beta_0 \\ 0 & \delta_0 & 0 & 0 \\ 0 & 0 & \delta_0 & 0 \\ \beta_0 & 0 & 0 & 0 \end{pmatrix} \tag{B25}$$

and in the latter case U_0 is self-dual unitary, of the canonical form given in Eq. (B5).

For two-qubit gates of the form given in Eq. (A1) without any restriction on the parameters, the general form of a two-qubit dual-unitary gate obtained from the map is

$$U_0 = \begin{pmatrix} \alpha_0 & 0 & 0 & \beta_0 \\ 0 & \pm\beta_0 & \pm\alpha_0 & 0 \\ 0 & \pm\alpha_0 & \pm\beta_0 & 0 \\ \beta_0 & 0 & 0 & \alpha_0 \end{pmatrix}.$$

APPENDIX C: DETAILS ABOUT THE MAP IN TERMS OF CARTAN PARAMETERS

1. Map in terms of Cartan parameters

a. XXX family

For $c_1^{(n)} = c_1^{(n)} = c_1^{(n)} = c^{(n)}$, the complex-number arguments appearing in Eq. (36) simplify to

$$\theta_+^{(n)} = -\arctan\left[\frac{1-\cos 2\,c^{(n)}}{1+\cos 2\,c^{(n)}}\tan c^{(n)}\right],$$
$$\theta_-^{(n)} = -\arctan\left[\frac{1+\cos 2\,c^{(n)}}{1-\cos 2\,c^{(n)}}\tan c^{(n)}\right],$$
$$\phi_+^{(n)} = -\arctan\left[\frac{1}{\tan c^{(n)}}\right],$$
$$\phi_-^{(n)} = \pi - \arctan\left[\frac{1}{\tan c^{(n)}}\right]. \tag{C1}$$

Using the above equation, Eq. (36) simplifies to

$$c_1^{(n+1)} = c_3^{(n+1)} = c^{(n+1)} = \frac{\pi}{4} - \frac{1}{4}\arctan\left[\frac{2}{\tan 2\,c^{(n)}}\right], \tag{C2}$$

for all n and

$$c_2^{(n+1)} = c^{(n+1)} \text{ for odd } n, = \frac{\pi}{2} - c^{(n+1)} \text{ for even } n, \tag{C3}$$

where the Cartan coefficients satisfy $0 \le c_3^{(n)} \le c_2^{(n)} \le c_1^{(n)}$ for all n. Thus the map on Cartan parameters is 1D and is given by

$$c^{(n+1)} = \frac{\pi}{4} - \frac{1}{4}\arctan\left[\frac{2}{\tan 2\,c^{(n)}}\right]. \tag{C4}$$

It is easy to check that $c^* = \pi/4$ is the fixed point of the map. We show that it is global attractor for all $c^{(0)} \in (0, \pi/4]$ below. In terms of $x_n = 1/\tan 2\ c^{(n)}$, Eq. (C4) becomes

$$x_n = \frac{x_{n+1}}{1 - x_{n+1}^2}, \tag{C5}$$

which, under rearrangement, gives Eq. (42).

To prove convergence, we write the map in terms of x_n defined in Eq. (41) as

$$\frac{x_{n+1}}{x_n} = \frac{2}{1 + \sqrt{(2\,x_n)^2 + 1}}. \tag{C6}$$

For $x_n \in (0, \infty)$, $1 < \sqrt{(2x_n)^2 + 1}$, hence we obtain

$$1 + \sqrt{(2\,x_n)^2 + 1} > 2 \implies \frac{2}{1 + \sqrt{(2\,x_n)^2 + 1}} < 1.$$

Hence, from Eq. C6, $x_{n+1} < x_n$ and this explains the contractive nature of the map. The convergence of the map can also be justified in terms of its Jacobian, given by

$$J_x = \frac{d}{dx}\left[\frac{2\,x}{1 + \sqrt{4\,x^2 + 1}}\right] = \frac{2}{1 + 4\,x^2 + \sqrt{1 + 4\,x^2}},$$

with $J_x < 1\ \forall\ x \in (0, \infty)$. The approach to the fixed point $x^* = 0$ or, equivalently, the approach of U_n to the SWAP

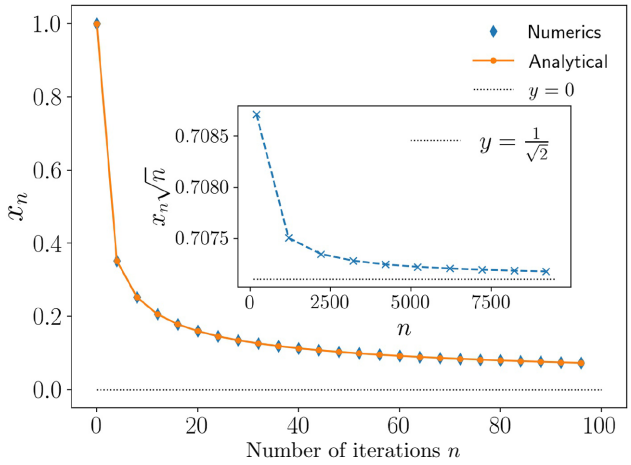

FIG. 14. The XXX case: convergence to the respective fixed point $x^* = 0$ under the map initiated with $c^{(0)} = \pi/8$ or, equivalently $x_0 = 1$. The inset shows the power-law behavior for the same initial condition, as seen from the convergence $x_n\sqrt{n} \to 1/\sqrt{2}$ for large n.

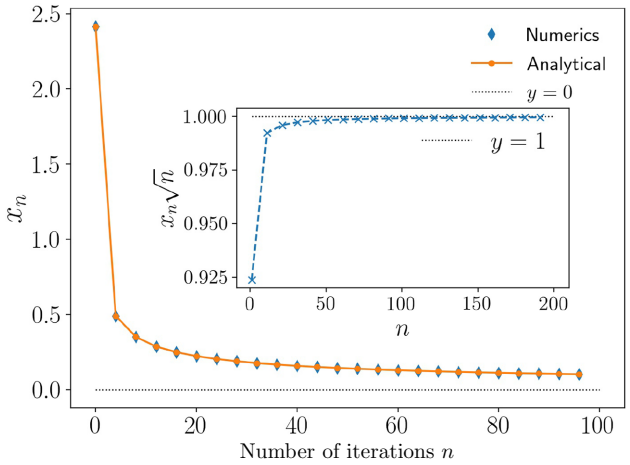

FIG. 15. The SWAP-CNOT edge: convergence to the respective fixed point $y^* = 0$ under the map initiated with $c^{(0)} = \pi/16$. The inset shows the power-law behavior for the same initial condition as seen from the convergence $y_n\sqrt{n} \to 1$ for large n.

gate, is *algebraic* with an exponent equal to $1/2$, as shown in Fig. 14 for $x_0 = 1$. The numerical values in Fig. 14 obtained from the algorithm proposed in Ref. [79] exactly match the analytical values obtained from Eq. (42).

b. SWAP-CNOT-DCNOT face

In this case, the substitution $c_1^{(n)} = \pi/4$ and assuming that $0 \le c_3^{(n)} \le c_2^{(n)} \le c_1^{(n)} \le \pi/4$ simplifies the complex-number arguments in the 3D map of Eq. (36) to

$$\begin{aligned}
\theta_+^{(n)} &= -\arctan\left[\tan c_2^{(n)} \tan c_3^{(n)}\right], \\
\theta_-^{(n)} &= -\arctan\left[\frac{\tan c_3^{(n)}}{\tan c_2^{(n)}}\right], \\
\phi_+^{(n)} &= -\arctan\left[\frac{1}{\tan c_2^{(n)} \tan c_3^{(n)}}\right], \\
\phi_-^{(n)} &= \pi - \arctan\left[\frac{\tan c_2^{(n)}}{\tan c_3^{(n)}}\right].
\end{aligned} \tag{C7}$$

Using the above set of equations in Eq. (36), the map on the Cartan coefficients reduces to

$$\begin{aligned}
c_1^{(n+1)} &= \frac{\pi}{4}, \\
c_2^{(n+1)} &= \frac{\pi}{4} \pm \frac{1}{2}\arctan\left[\sin 2\, c_3^{(n)} \cot 2\, c_2^{(n)}\right], \\
c_3^{(n+1)} &= \frac{1}{2}\arctan\left[\frac{\tan 2\, c_3^{(n)}}{\sin 2c_2^{(n)}}\right].
\end{aligned} \tag{C8}$$

Thus the map is 2D and in terms of $y_n = 1/\tan^2 2\, c_2^{(n)}$ and $z_n = 1/\tan^2 2\, c_3^{(n)}$, the above 2D map takes a purely algebraic form given by Eq. (45) in the main text.

c. SWAP-CNOT edge

In this case, the map on the Cartan parameters is 1D: $c_1^{(n+1)} = \pi/4, c_2^{(n+1)} = c_3^{(n+1)} = c^{(n+1)}$, given by

$$c^{(n+1)} = \frac{1}{2}\arctan\left[\frac{1}{\cos 2\, c^{(n)}}\right]. \tag{C9}$$

In terms of $t_n = \tan^2(2\, c^{(n)})$, the above map takes a simple linear form

$$t_{n+1} = 1 + t_n; \tag{C10}$$

hence, $t_n = n - 1 + t_0$. In terms of $y_n = 1/\tan^2(2\ c^{(n)})$, this reduces to Eq. (53), with an exact solution given by Eq. (54). In this case, the approach to the fixed point $y^* = 0$ or, equivalently, the approach of U_n to the SWAP gate, is *algebraic* with an exponent equal to $1/2$, as shown in Fig. 15.

APPENDIX D: 2-UNITARIES WITH ENTANGLED ROWS AND COLUMNS

We write unitary operator U in block form as $U = \sum_{i,j=1}^{d} |i\rangle\langle j| \otimes X_{ij}$:

(1) Unitarity of U, expressed as $UU^\dagger = U^\dagger U = \mathbb{I}_{d^2}$:

$$UU^\dagger = \left(\sum_{i,j=1}^{d} |i\rangle\langle j| \otimes X_{ij}\right)\left(\sum_{k,l=1}^{d} |k\rangle\langle l| \otimes X_{kl}\right)^\dagger, \\ = \sum_{i,k=1}^{d}\left(|i\rangle\langle k| \otimes \sum_{j=1}^{d} X_{ij}X_{kj}^\dagger\right).$$

$UU^\dagger = \mathbb{I}_{d^2}$ gives

$$\sum_{j=1}^{d} X_{ij}X_{kj}^\dagger = \delta_{ik}\mathbb{I}_d. \tag{D1}$$

(2) Dual unitarity of U, expressed as $U^R U^{R\,\dagger} = U^{R\,\dagger}U^R = \mathbb{I}_{d^2}$:

$$U^R U^{R\,\dagger} = \left(\sum_{ij} |ij\rangle\langle X_{ij}^*|\right)\left(\sum_{kl} |kl\rangle\langle X_{kl}^*|\right)^\dagger, \\ = \sum_{ij}\sum_{kl}\langle X_{kl}|X_{ij}\rangle\, |ij\rangle\langle kl|.$$

$U^R U^{R\,\dagger} = \mathbb{I}_{d^2}$ gives

$$\langle X_{kl}|X_{ij}\rangle = \delta_{ik}\delta_{jl}, \tag{D2}$$

i.e., the X_{ij} form an orthonormal operator basis.

(3) T duality of U, expressed as $U^\Gamma U^{\Gamma\,\dagger} = \mathbb{I}_{d^2}$:

$$U^\Gamma U^{\Gamma\,\dagger} = \left(\sum_{i,j=1}^{d} |j\rangle\langle i| \otimes X_{ij}\right)\left(\sum_{k,l=1}^{d} |l\rangle\langle k| \otimes X_{kl}\right)^\dagger, \\ = \sum_{j,l=1}^{d}\left(|j\rangle\langle l| \otimes \sum_{i=1}^{d} X_{ij}X_{il}^\dagger\right).$$

$U^\Gamma U^{\Gamma\,\dagger} = \mathbb{I}_{d^2}$ gives

$$\sum_{i=1}^{d} X_{ij}X_{il}^\dagger = \delta_{jl}\mathbb{I}_d. \tag{D3}$$

The above conditions are equivalent to those presented in Refs. [56,96] in terms of single-qudit reduced-density matrices (marginals) of a two-qudit pure state: $X_{ij} \mapsto |X_{ij}\rangle = (X_{ij} \otimes \mathbb{I})\,|\Phi\rangle$, where $|\Phi\rangle$ is the generalized Bell state. It is easy to see that the marginal with respect to the first qudit is given by $X_{ij}X_{ij}^\dagger$. Thus conditions (1) and (2) above involve orthonormality of sums of single-qudit marginals in each row and each column, respectively. A $d \times d$ arrangement of d^2-dimensional vectors (two-qudit quantum states) $|X_{ij}\rangle$ that satisfy Eqs. (D1)–(D3) form an OQLS. This generalizes the notion of OLS for general 2-unitary operators that are not necessarily permutations or those for which single-qudit marginals are projectors, where each $|X_{ij}\rangle$ is a product state. The original definitions of OQLS [59,86] are fragile in the sense that they do not work when the $|X_{ij}\rangle$ are entangled. Note that the entanglement of two-qudit states $|X_{ij}\rangle$ changes when unitary $U = \sum_{i,j=1}^{d} |i\rangle\langle j| \otimes X_{ij}$ is multiplied by local unitary transformations.

APPENDIX E: FIXED POINT OF $\mathcal{M}_R^2$ MAP THAT IS NOT DUAL UNITARY

Here, we give an example of a fixed point of the $\mathcal{M}_R^2$ map in $d^2 = 9$ that is not dual unitary. The unitary is given by

$$U_{\mathrm{ND}} = \begin{pmatrix} 1 & 0 & 0 & 0 & 0 & 0 & 0 & 0 & 0 \\ 0 & 0 & \sqrt{3}/2 & 1/2 & 0 & 0 & 0 & 0 & 0 \\ 0 & 0 & 0 & 0 & 0 & \sqrt{3}/2 & -1/2 & 0 & 0 \\ 0 & 0 & 0 & 0 & 0 & 0 & 0 & 1 & 0 \\ 0 & 1 & 0 & 0 & 0 & 0 & 0 & 0 & 0 \\ 0 & 0 & 0 & 0 & 1 & 0 & 0 & 0 & 0 \\ 0 & 0 & 0 & 0 & 0 & 0 & 0 & 0 & 1 \\ 0 & 0 & -1/2 & \sqrt{3}/2 & 0 & 0 & 0 & 0 & 0 \\ 0 & 0 & 0 & 0 & 0 & 1/2 & \sqrt{3}/2 & 0 & 0 \end{pmatrix}. \tag{E1}$$

The action of $\mathcal{M}_R$ map on U_{ND} results in

$$U'_{\mathrm{ND}} := \mathcal{M}_R[U_{\mathrm{ND}}] \tag{E2}$$

$$= \begin{pmatrix} \sqrt{3}/2 & 0 & 0 & 0 & 0 & 1/2 & 0 & 0 & 0 \\ 0 & 0 & 0 & 0 & 0 & 0 & 0 & 0 & 1 \\ 0 & 0 & 1/2 & 0 & 0 & 0 & -\sqrt{3}/2 & 0 & 0 \\ 0 & 0 & 0 & 0 & 1 & 0 & 0 & 0 & 0 \\ 0 & 0 & 0 & 0 & 0 & 0 & 0 & 1 & 0 \\ 0 & 1 & 0 & 0 & 0 & 0 & 0 & 0 & 0 \\ 1/2 & 0 & 0 & 0 & 0 & -\sqrt{3}/2 & 0 & 0 & 0 \\ 0 & 0 & 0 & 1 & 0 & 0 & 0 & 0 & -0 \\ 0 & 0 & \sqrt{3}/2 & 0 & 0 & 0 & 1/2 & 0 & 0 \end{pmatrix}, \tag{E3}$$

such that $\mathcal{M}_R[U'_{\mathrm{ND}}] = U_{\mathrm{ND}}$, i.e., U_{ND} (the subscript "ND" is used to emphasize it is not dual unitary) is a fixed point of the $\mathcal{M}_R^2$ map

$$\mathcal{M}_R^2[U_{\mathrm{ND}}] := \mathcal{M}_R[\mathcal{M}_R[U_{\mathrm{ND}}]] = \mathcal{M}_R[U'_{\mathrm{ND}}] = U_{\mathrm{ND}}.$$

Interestingly, U_{ND} and U'_{ND} are LU equivalent,

$$U_{\mathrm{ND}} = (u_1 \otimes u_2)U'_{\mathrm{ND}}(v_1 \otimes v_2), \tag{E4}$$

where

$$u_1 = \begin{pmatrix} -\sqrt{3}/2 & 0 & -1/2 \\ 0 & 1 & 0 \\ -1/2 & 0 & \sqrt{3}/2 \end{pmatrix}, \; u_2 = v_1 = \begin{pmatrix} 1 & 0 & 0 \\ 0 & 0 & 1 \\ 0 & -1 & 0 \end{pmatrix},$$

$$\text{and } v_2 = \begin{pmatrix} -1 & 0 & 0 \\ 0 & 1 & 0 \\ 0 & 0 & -1 \end{pmatrix}.$$

U_{ND} (U'_{ND}) is not dual unitary: $U^R_{\mathrm{ND}} U^{R\,\dagger}_{\mathrm{ND}} \neq \mathbb{I}$, having three distinct Schmidt values given by $\{1+\sqrt{3}/2, 1, 1-\sqrt{3}/2\}$, with each value repeated three times. As a consequence of LU equivalence, U_{ND} and U'_{ND} have the same entangling power and gate typicality.

[1] L. Amico, R. Fazio, A. Osterloh, and V. Vedral, Entanglement in many-body systems, Rev. Mod. Phys. **80**, 517 (2008).

[2] B. Zeng, X. Chen, D.-L. Zhou, and X.-G. Wen, Quantum information meets quantum matter—from quantum entanglement to topological phase in many-body systems (2015), arXiv preprint ArXiv:1508.02595.

[3] A. Jahn and J. Eisert, Holographic tensor network models and quantum error correction: A topical review, Quantum Science and Technology (2021).

[4] T. Kibe, P. Mandayam, and A. Mukhopadhyay, Holographic spacetime, black holes and quantum error correcting codes: A review (2021), arXiv preprint ArXiv:2110.14669.

[5] R. P. Feynman, in *Feynman and computation* (CRC Press, 2018), p. 133.

[6] I. M. Georgescu, S. Ashhab, and Fr. Nori, Quantum simulation, Rev. Mod. Phys. **86**, 153 (2014).

[7] J. Preskill, Quantum computing in the NISQ era and beyond, Quantum **2**, 79 (2018).

[8] M. Ippoliti, K. Kechedzhi, R. Moessner, S. L. Sondhi, and V. Khemani, Many-Body Physics in the NISQ Era: Quantum Programming a Discrete Time Crystal, PRX Quantum **2**, 030346 (2021).

[9] F. Arute, K. Arya, R. Babbush, D. Bacon, J. C. Bardin, R. Barends, R. Biswas, S. Boixo, F. G. S. L. Brandao, and D. A. Buell, *et al.*, Quantum supremacy using a programmable superconducting processor, Nature **574**, 505 (2019).

[10] Q. Zhu, S. Cao, F. Chen, M.-C. Chen, X. Chen, T.-H. Chung, H. Deng, Y. D. Daojin Fan, and M. Gong, *et al.*, Quantum computational advantage via 60-qubit 24-cycle random circuit sampling, Science Bulletin (2021).

[11] A. Nahum, S. Vijay, and J. Haah, Operator Spreading in Random Unitary Circuits, Phys. Rev. X **8**, 021014 (2018).

[12] A. Nahum, J. Ruhman, S. Vijay, and J. Haah, Quantum Entanglement Growth under Random Unitary Dynamics, Phys. Rev. X **7**, 031016 (2017).

[13] V. Khemani, A. Vishwanath, and D. A. Huse, Operator Spreading and the Emergence of Dissipative Hydrodynamics under Unitary Evolution with Conservation Laws, Phys. Rev. X **8**, 031057 (2018).

[14] C. W. Von Keyserlingk, T. Rakovszky, F. Pollmann, and S. L. Sondhi, Operator Hydrodynamics, OTOCs, and Entanglement Growth in Systems without Conservation Laws, Phys. Rev. X **8**, 021013 (2018).

[15] A. Chan, A. De Luca, and J. T. Chalker, Solution of a Minimal Model for Many-Body Quantum Chaos, Phys. Rev. X **8**, 041019 (2018).

[16] M. Akila, D. Waltner, B. Gutkin, and T. Guhr, Particle-time duality in the kicked Ising spin chain, J. Phys. A: Math. Theor. **49**, 375101 (2016).

[17] B. Bertini, P. Kos, and T. Prosen, Exact Correlation Functions for Dual-Unitary Lattice Models in 1 + 1 Dimensions, Phys. Rev. Lett. **123**, 210601 (2019).

[18] B. Gutkin, P. Braun, M. Akila, D. Waltner, and T. Guhr, Exact local correlations in kicked chains, Phys. Rev. B **102**, 174307 (2020).

[19] P. Braun, D. Waltner, M. Akila, B. Gutkin, and T. Guhr, Transition from quantum chaos to localization in spin chains, Phys. Rev. E **101**, 052201 (2020).

[20] B. Bertini, P. Kos, and T. Prosen, Exact Spectral Form Factor in a Minimal Model of Many-Body Quantum Chaos, Phys. Rev. Lett. **121**, 264101 (2018).

[21] B. Bertini, P. Kos, and T. Prosen, Entanglement Spreading in a Minimal Model of Maximal Many-Body Quantum Chaos, Phys. Rev. X **9**, 021033 (2019).

[22] B. Bertini, P. Kos, and T. Prosen, Operator entanglement in local quantum circuits I: Chaotic dual-unitary circuits, SciPost Phys. **8**, 067 (2020).

[23] P. Kos, B. Bertini, and T. Prosen, Chaos and Ergodicity in Extended Quantum Systems with Noisy Driving, Phys. Rev. Lett. **126**, 190601 (2021).

[24] A. Lerose, M. Sonner, and D. A. Abanin, Influence Matrix Approach to Many-Body Floquet Dynamics, Phys. Rev. X **11**, 021040 (2021).

[25] S. J. Garratt and J. T. Chalker, Local Pairing of Feynman Histories in Many-Body Floquet Models, Phys. Rev. X **11**, 021051 (2021).

[26] A. Flack, B. Bertini, and T. Prosen, Statistics of the spectral form factor in the self-dual kicked Ising model, Phys. Rev. Res. **2**, 043403 (2020).

[27] B. Bertini, P. Kos, and T. Prosen, Operator entanglement in local quantum circuits II: Solitons in chains of qubits, SciPost Phys. **8**, 068 (2020).

[28] L. Piroli, B. Bertini, J. Ignacio Cirac, and T. Prosen, Exact dynamics in dual-unitary quantum circuits, Phys. Rev. B **101**, 094304 (2020).

[29] P. W. Claeys and A. Lamacraft, Maximum velocity quantum circuits, Phys. Rev. Res. **2**, 033032 (2020).

[30] K. Klobas, B. Bertini, and L. Piroli, Exact Thermalization Dynamics in the "Rule 54" Quantum Cellular Automaton, Phys. Rev. Lett. **126**, 160602 (2021).

[31] M. Ippoliti, T. Rakovszky, and V. Khemani, Fractal, Logarithmic, and Volume-Law Entangled Nonthermal Steady States via Spacetime Duality, Phys. Rev. X **12**, 011045 (2022).

[32] M. Ippoliti and V. Khemani, Postselection-Free Entanglement Dynamics via Spacetime Duality, Phys. Rev. Lett. **126**, 060501 (2021).

[33] K. Klobas and B. Bertini, Entanglement dynamics in rule 54: Exact results and quasiparticle picture, SciPost Phys. **11**, 107 (2021).

[34] P. W. Claeys and A. Lamacraft, Emergent quantum state designs and biunitarity in dual-unitary circuit dynamics (2022), arXiv preprint ArXiv:2202.12306.

[35] T. Zhou and A. W. Harrow, Maximal entanglement velocity implies dual unitarity (2022),.

[36] P. Zanardi, C. Zalka, and L. Faoro, Entangling power of quantum evolutions, Phys. Rev. A **62**, 030301 (2000).

[37] P. Zanardi, Entanglement of quantum evolutions, Phys. Rev. A **63**, 040304 (2001).

[38] X. Wang and P. Zanardi, Quantum entanglement of unitary operators on bipartite systems, Phys. Rev. A **66**, 044303 (2002).

[39] X. Wang, B. C. Sanders, and D. W. Berry, Entangling power and operator entanglement in qudit systems, Phys. Rev. A **67**, 042323 (2003).

[40] M. A. Nielsen, C. M. Dawson, J. L. Dodd, A. Gilchrist, D. Mortimer, T. J. Osborne, M. J. Bremner, A. W. Harrow, and A. Hines, Quantum dynamics as a physical resource, Phys. Rev. A **67**, 052301 (2003).

[41] G. Vidal and J. I. Cirac, Catalysis in Nonlocal Quantum Operations, Phys. Rev. Lett. **88**, 167903 (2002).

[42] K. Hammerer, G. Vidal, and J. I. Cirac, Characterization of nonlocal gates, Phys. Rev. A **66**, 062321 (2002).

[43] D. Collins, N. Linden, and S. Popescu, Nonlocal content of quantum operations, Phys. Rev. A **64**, 032302 (2001).

[44] J. Eisert, K. Jacobs, P. Papadopoulos, and M. B. Plenio, Optimal local implementation of nonlocal quantum gates, Phys. Rev. A **62**, 052317 (2000).

[45] J. I. Cirac, W. Dür, B. Kraus, and M. Lewenstein, Entangling Operations and Their Implementation Using a Small Amount of Entanglement, Phys. Rev. Lett. **86**, 544 (2001).

[46] M. R. Dowling and M. A. Nielsen, The geometry of quantum computation, Quantum Inf. Comput. **8**, 861 (2008).

[47] S. A. Rather, S. Aravinda, and A. Lakshminarayan, Creating Ensembles of Dual Unitary and Maximally Entangling Quantum Evolutions, Phys. Rev. Lett. **125**, 070501 (2020).

[48] D. Goyeneche, D. Alsina, J. I. Latorre, A. Riera, and K. Życzkowski, Absolutely maximally entangled states, combinatorial designs, and multiunitary matrices, Phys. Rev. A **92**, 032316 (2015).

[49] F. Pastawski, B. Yoshida, D. Harlow, and J. Preskill, Holographic quantum error-correcting codes: Toy models for the bulk/boundary correspondence, J. High Energy Phys. **2015**, 149 (2015).

[50] S. Aravinda, S. A. Rather, and A. Lakshminarayan, From dual-unitary to quantum Bernoulli circuits: Role of the entangling power in constructing a quantum ergodic hierarchy, Phys. Rev. Res. **3**, 043034 (2021).

[51] J. E. Tyson, Operator-schmidt decompositions and the Fourier transform, with applications to the operator-Schmidt numbers of unitaries, J. Phys. A: Math. Gen. **36**, 10101 (2003).

[52] J. Tyson, Operator-Schmidt decomposition of the quantum Fourier transform on $\mathbb{C}^{N_1} \otimes \mathbb{C}^{N_2}$, J. Phys. A: Math. Gen. **36**, 6813 (2003).

[53] B. Jonnadula, P. Mandayam, K. Życzkowski, and A. Lakshminarayan, Entanglement measures of bipartite quantum gates and their thermalization under arbitrary interaction strength, Phys. Rev. Res. **2**, 043126 (2020).

[54] P. W. Claeys and A. Lamacraft, Ergodic and Nonergodic Dual-Unitary Quantum Circuits with Arbitrary Local Hilbert Space Dimension, Phys. Rev. Lett. **126**, 100603 (2021).

[55] S. Singh and I. Nechita, Diagonal unitary and orthogonal symmetries in quantum theory II: Evolution operators (2021), arXiv preprint ArXiv:2112.11123.

[56] S. A. Rather, A. Burchardt, W. Bruzda, G. Rajchel-Mieldzioć, A. Lakshminarayan, and K. Życzkowski, Thirty-Six Entangled Officers of Euler: Quantum Solution to a Classically Impossible Problem, Phys. Rev. Lett. **128**, 080507 (2022).

[57] K. Życzkowski, W. Bruzda, G. Rajchel-Mieldzioć, A. Burchardt, S. A. Rather, and A. Lakshminarayan, $9 \times 4 = 6 \times 6$: Understanding the quantum solution to the Euler's problem of 36 officers (2022),.

[58] W. Helwig, W. Cui, J. I. Latorre, A. Riera, and H. K. Lo, Absolute maximal entanglement and quantum secret sharing, Phys. Rev. A **86**, 052335 (2012).

[59] D. Goyeneche, Z. Raissi, S. Di Martino, and K. Życzkowski, Entanglement and quantum combinatorial designs, Phys. Rev. A **97**, 062326 (2018).

[60] L. Clarisse, S. Ghosh, S. Severini, and A. Sudbery, Entangling power of permutations, Phys. Rev. A **72**, 012314 (2005).

[61] A. Burchardt and Z. Raissi, Stochastic local operations with classical communication of absolutely maximally entangled states, Phys. Rev. A **102**, 022413 (2020).

[62] B. Jonnadula, P. Mandayam, K. Życzkowski, and A. Lakshminarayan, Impact of local dynamics on entangling power, Phys. Rev. A **95**, 040302 (2017).

[63] A. Ocneanu, Quantized groups, string algebras and Galois theory for algebras, Oper. Algebra Appl. **2**, 119 (1988).

[64] U. Krishnan and V. Sunder, On biunitary permutation matrices and some subfactors of index 9, Trans. Am. Math. Soc. **348**, 4691 (1996).

[65] V. F. R. Jones, Planar algebras, I (1999), arXiv preprint ArXiv:math/9909027.

[66] D. J. Reutter and J. Vicary, Biunitary constructions in quantum information (2016), arXiv preprint ArXiv:1609.07775.

[67] T. Benoist and I. Nechita, On bipartite unitary matrices generating subalgebra-preserving quantum operations, Linear Algebra Appl. **521**, 70 (2017).

[68] V. Kodiyalam, Sruthymurali, and V. S. Sunder, Planar algebras, quantum information theory and subfactors, Int. J. Math. **31**, 2050124 (2020).

[69] I. Nechita, S. Schmidt, and M. Weber, Sinkhorn algorithm for quantum permutation groups, Experimental Mathematics **0**, 1 (2021).

[70] B. Gutkin and V. Osipov, Classical foundations of many-particle quantum chaos, Nonlinearity **29**, 325 (2016).

[71] K. Fan and A. J. Hoffman, Some metric inequalities in the space of matrices, Proc. Am. Math. Soc. **6**, 111 (1955).

[72] J. B. Keller, Closest unitary, orthogonal and Hermitian operators to a given operator, Math. Mag. **48**, 192 (1975).

[73] T. Benoist and I. Nechita, On bipartite unitary matrices generating subalgebra-preserving quantum operations, Linear Algebra Appl. **521**, 70 (2017).

[74] G. Rajchel-Mieldzioć, Quantum mappings and designs (2022),.

[75] T. Prosen, Many-body quantum chaos and dual-unitarity round-a-face? Chaos: An Interdiscip. J. Nonlinear Sci. **31**, 093101 (2021).
[76] N. Khaneja, R. Brockett, and S. J. Glaser, Time optimal control in spin systems, Phys. Rev. A **63**, 032308 (2001).
[77] B. Kraus and J. I. Cirac, Optimal creation of entanglement using a two-qubit gate, Phys. Rev. A **63**, 062309 (2001).
[78] J. Zhang, J. Vala, S. Sastry, and K. B. Whaley, Geometric theory of nonlocal two-qubit operations, Phys. Rev. A **67**, 042313 (2003).
[79] M. Musz, M. Kuś, and K. Życzkowski, Unitary quantum gates, perfect entanglers, and unistochastic maps, Phys. Rev. A **87**, 022111 (2013).
[80] A. M. Childs, H. L. Haselgrove, and M. A. Nielsen, Lower bounds on the complexity of simulating quantum gates, Phys. Rev. A **68**, 052311 (2003).
[81] M. Vanicat, L. Zadnik, and T. Prosen, Integrable Trotterization: Local Conservation Laws and Boundary Driving, Phys. Rev. Lett. **121**, 030606 (2018).
[82] A. Mandarino, T. Linowski, and K. Życzkowski, Bipartite unitary gates and billiard dynamics in the Weyl chamber, Phys. Rev. A **98**, 012335 (2018).
[83] A. D. Keedwell and J. Dénes, *Latin Squares and Their Applications* (Elsevier, Amsterdam, Netherlands, 2015).
[84] R. C. Bose, S. S. Shrikhande, and E. T. Parker, Further results on the construction of mutually orthogonal Latin squares and the falsity of Euler's conjecture, Can. J. Math. **12**, 189 (1960).
[85] B. Musto and J. Vicary, Quantum Latin squares and unitary error bases, Quantum Info. Comput. **16**, 1318 (2016).
[86] B. Musto and J. Vicary, Orthogonality for quantum Latin isometry squares, Electron. Proc. Theor. Comput. Sci. **287**, 253 (2019).
[87] J. Paczos, M. Wierzbiński, G. Rajchel-Mieldzioć, A. Burchardt, and K. Życzkowski, Genuinely quantum solutions of the game sudoku and their cardinality, Phys. Rev. A **104**, 042423 (2021).
[88] I. Nechita and J. Pillet, Sudoq—a quantum variant of the popular game (2020), arXiv preprint ArXiv:2005.10862.
[89] M. Borsi and B. Pozsgay, Remarks on the construction and the ergodicity properties of dual unitary quantum circuits (with an appendix by Roland Bacher and Denis Serre) (2022), arXiv preprint ArXiv:2201.07768.
[90] J. Chen, R. Duan, Z. Ji, M. Ying, and J. Yu, Existence of universal entangler, J. Math. Phys. **49**, 012103 (2008).
[91] F. V. Mendes and R. V. Ramos, Numerical search for universal entanglers in $c^3 \otimes c^4$ and $c^4 \otimes c^4$, Phys. Lett. A **379**, 289 (2015).
[92] N. J. A. Sloane, and The OEIS Foundation Inc., The on-line encyclopedia of integer sequences (2020).
[93] Z. Raissi, A. Teixidó, C. Gogolin, and A. Acín, Constructions of k-uniform and absolutely maximally entangled states beyond maximum distance codes, Phys. Rev. Res. **2**, 033411 (2020).
[94] U. Krishnan and V. S. Sunder, On biunitary permutation matrices and some subfactors of index 9, Trans. Am. Math. Soc. **348**, 4691 (1996).
[95] V. Kodiyalam and V. S. Sunder, A complete set of numerical invariants for a subfactor, J. Funct. Anal. **212**, 1 (2004).
[96] A. Rico, Master's thesis, Institute for theoretical physics, University of Innsbruck (2020).